The Pennsylvania State University

The Graduate School

Department of Mechanical and Nuclear Engineering

DESIGN FOR IN-LINE PIPE INSPECTION USING

ULTRASONIC GUIDED WAVES

A Thesis in

Mechanical Engineering

by

Matthew S. Lindsey

Submitted in Partial Fulfillment
of the Requirements
for the Degree of

Master of Science

May 2011

The thesis of Matthew S. Lindsey was reviewed and approved* by the following:

Joseph L. Rose
Paul Morrow Professor of Engineering Science and Mechanics
Thesis Co-Advisor

Jack Brenizer
J. Lee Everett Professor of Mechanical and Nuclear Engineering
Thesis Co-Advisor

Panagiotis Michaleris
Associate Professor of Mechanical Engineering

Dr. Karen A. Thole
Professor of Mechanical Engineering
Department Head of Mechanical and Nuclear Engineering

*Signatures are on file in the Graduate School

ABSTRACT

Inline pipe inspection tools and techniques can richly utilize Ultrasonic Guided Wave technology. This technology could also be used to supplement other in line inspection devices currently in use. Different applications and types of defect detection will be explored. This was done by experimentation and the use of different sensor designs. The impact of different sensor designs for the inspection of deep gas storage well and gas distribution lines were explored. Results from the different sensors will be presented and analyzed. The technology and sensors developed were implemented into prototype designs of in line guided wave inspection tools. The designs were able to classify and size different defects using both circumferential and longitudinal direction guided waves. Circular pitting depth was estimated using pulse echo and through transmission type sensors. A result of different hardware designs, improved methods, and analysis techniques allowed the initial prototypes to successfully detect and size defects.

TABLE OF CONTENTS

LIST OF FIGURES

LIST OF TABLES

ACKNOWLEDGEMENTS

I would like to thank my family for always providing me with words of encouragement and support throughout my education.

I would like to thank Dr. Joseph Rose for providing me with the opportunity to do this work. Words can not describe my thankfulness. Without his guidance none of this work would have been possible.

FBS Inc. and all of its employees also made this work possible. I want to thank everyone for allowing me to use the company's resources, Dr. Jason Van Velsor, for his guidance, advice, and work on all projects, and Russell Love for his vast programming knowledge and support.

I also could not ask for a better supervisor at FBS Inc. than Steve Owens who has helped me throughout my early career. His knowledge and guidance has been a great help.

In particular, thanks for special contributions to this thesis are given to. Jason Van Velsor for dispersion curve computations, Steve Owens for design approval, Ron Then and Ehsan Khajeh for laboratory help, and Russell Love for software support.

A special thanks for financial support from FBS Inc. and the Gas Storage Technology Consortium (GSTC).

Chapter 1

INTRODUCTION

1.1 Motivation

Many pipelines are critical components in a system. If the system is not in good working condition, catastrophic failure could occur. A safety system could fail because of a defect or corrosion in a pipe. A malfunction in a pipeline, due to corrosion, could lead to a reduction or loss of profits in the energy sector. Some of these pipes cannot be inspected visually or through any current ultrasonic method because of limited pipe access. A gas storage well casing is constructed in such a way that pipe access is often very limited [GE Oil and Gas, 2010]. A robust, economical, and reliable way to inspect the integrity of a gas storage casing is needed. Ultrasonic Guided Waves lend themselves well to the solution of this problem. The current method used for inspecting gas storage wells is using a MFL PIG (magnetic flux leakage, pipe inspection gauge) [GE Oil & Gas].

This is an inline inspection tool that is widely used on accessible pipelines. Gas storage wells have only one access, the well head, being both the inlet and outlet. Being able to analyze the integrity of the well casing is key to having a successful operating storage well. The main component of the casing is a steel pipe. If the casing has a crack, corrosion or any defects, gas could leak and be lost. When gas is leaked through the casing this can cause environmental problems and an undesirable loss of gas.

One other area of interest is being able to detect pitting corrosion. This is an area of great interest because it can lead to failure for gas distribution lines [Papavinasam, S., 2009]. High reliability is needed.

1.2 Current Pipeline Inspection Methods

Current methods are not sufficient for accuracy and cost effectiveness, or not even possible to use. Table 1.1 shows current methods along with limitations. Bulk wave ultrasonics need to have complete circumferential pipe access for the desired section of the pipeline to be inspected. For stationary guided wave ultrasonics, the energy of the wave will only travel so far. Depending on the pipe conditions, this could be hundreds of feet, or 5 feet. In the case of buried and tar coated pipelines, the signal could be so attenuated and distorted that test results are inconclusive. The most current method used to inspect long distances of inaccessible pipeline is Magnetic Flux Leakage (MFL) [GE Drilling and Production, 2010].

Table **1.1** Current NDT (Non Destructive Testing) techniques and their limitations.

Current NDT technique	**Limitations**
bulk wave	time consuming
guided wave (stationary)	Pipeline access needed
MFL	Can not detect all defects (considered mature technology)

1.2.1 Bulk Wave Ultrasonics

Bulk waves propagate in infinite media. A boundary is not required for their existence.[Rose, 1999] The longitudinal bulk wave velocity for steel is 5850 m/s, and the shear wave velocity is 3230 m/s. [Rose, 1999] Bulk waves can be used for point by point thickness measurements of a pipeline wall thickness. To inspect a large section of pipeline in this fashion is not very practical. In order to use the guided wave method full circumferential access to the pipe is needed. This NDT inspection method would be acceptable in an accessible pipe or in the event of a pipe appearance after excavation. In this case one would then have complete access to the pipe. Using bulk waves over guided waves would mean more excavations and disturbances to pipelines that may not be needed.

One can use either a pulse-echo mode or through transmission mode. Pulse-echo is when the ultrasonic signal is sent and received from the same position. Through transmission is when the ultrasonic signal is generated in one position and sent to a receiver somewhere else.

Wavelength can be calculated as a function of the input frequency f and wave velocity c. The wave velocity is a characteristic of the material.

$$c = f \lambda$$

Ultrasonic wave frequencies are normally used in the range from 40 kHz to 500MHz. [Rose, 1999]

1.2.2 Guided Wave Ultrasonics

Guided waves are ultrasonic waves that require a boundary for their existence. There are many types of guided waves such as surface waves, Lamb waves, and shear horizontal waves. The types used within this research are shear horizontal, and Lamb type waves.

Shear horizontal waves, more commonly called torsional waves in pipes are time harmonic wave motions. The particle vibrations occur in a plane that is parallel to the surfaces of the flat layer. If a wave vector is in the X_1 direction then the particle displacements are in the X_3 direction as shown in Figure 1.1.

The Lamb type waves occur when ultrasonic excitation occurs at some point on a plate. The longitudinal wave vector is in the X_1 direction, particle velocity is in the X_1 and X_2 directions. Mode conversion occurs with longitudinal and shear waves. After some travel, wave packets are formed and are the guided wave modes. Based on the entry angle and the frequency used, the number of different modes that can be produced in a plate can be predicted.

There are many ways to produce these types of guided waves and more details are given in subsequent chapters.

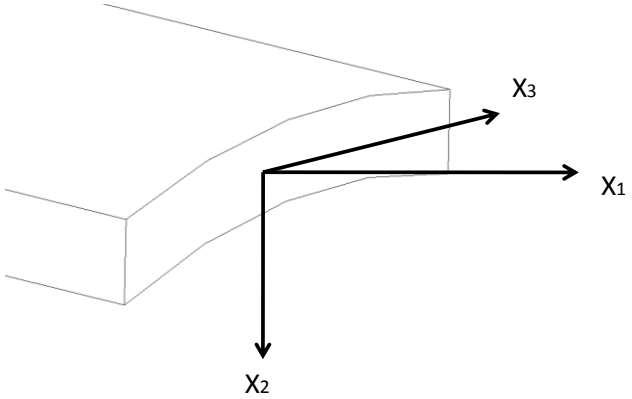

Figure 1.1 A Coordinate system to depict wave vector and particle displacement directions for different types of guided waves.

1.2.3 Magnetic Flux Leakage

The most current method used to inspect long distances of an inaccessible pipeline is Magnetic Flux Leakage (MFL). This method has high tolerances and relatively low certainty and confidence with certain pipeline anomalies such as corrosion [FBS Inc., 2010]. Table 1.2 shows current MFL capabilities. With an MFL tool the probability of corrosion detection is only 80% [GE Oil and Gas, 2010]. For the corrosion to be detected it has to be at least 10% through the wall thickness. Tolerance on width and length size prediction of corrosion is ± 0.787". [GE Oil and Gas, 2010] With these kinds of specifications there are quite a few small corrosion spots that could be missed. Guided waves could greatly improve the reliability and confidence of these inspections. With this type of ultrasonic inspection, only an inlet and outlet of the tool is needed. A guided wave tool can be potentially implemented into an MFL tool; long distance use with minimal disturbance to the system is possible. Such an approach would result in minimal downtime, and be cost effective. Also, allowing hundreds of feet of pipe to be inspected, in a short amount of time with higher accuracy.

Table **1.2** Current MFL tool capabilities where; WT = wall thickness and POD = probability of detection. [2]

Mechanical Damage	**Corrosion**
minimum size 2% of pipe diameter	min. depth 10% WT
90% POD	80% POD
	±.787" width and length

1.3 Proposed inspection solution

The proposed solution to well steel pipe casing inspection is a tool that can be lowered down the casing. It will use guided waves to detect anomalies in the longitudinal and circumferential direction. Corrosion or pitting is an anomaly that by classification falls into both groups and will also be detected. The proposed solution is to use shear horizontal guided waves, in deep gas well storage, and Lamb type waves for pitting detection in gas distribution lines. Both types of guided waves will be generated using an EMAT (Electro Magnetic Acoustic Transducer).

An EMAT type sensor was chosen because of the ease of generating guided waves in the material. Other methods, such as an angle beam wedge as shown in Figure 1.1, would need couplant. The couplant is used to transfer the energy from the plexiglass material into the material being inspected.

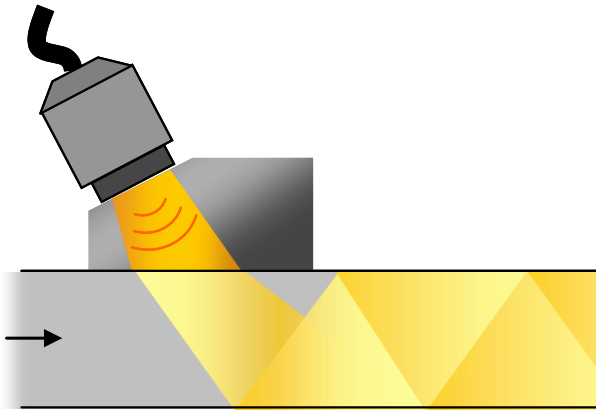

Figure 1.2 A depiction of the angle beam wedge method. [FBS Inc., 2010]

If using an angle beam method one would chose a desired frequency and phase velocity. Then the angle of the wedge would be determined by using Snell's law.

$$c_1 \sin\theta_2 = c_2 \sin\theta_1$$ [Rose, 1999]

Here c_1 is the velocity of sound in plexiglass, the wedge material, c_2 is the velocity in the inspection material, and θ is the angle of incidence in the wedge. c_2 is the phase velocity in the test material and θ_2 is 90°.

An EMAT transducer shown in Figure 1.2 lends itself well to the problem because of its non contact nature. There is no couplant needed to induce the guided waves into the pipe. This would reduce the need for extra subsystems in the design, such as bubblers.

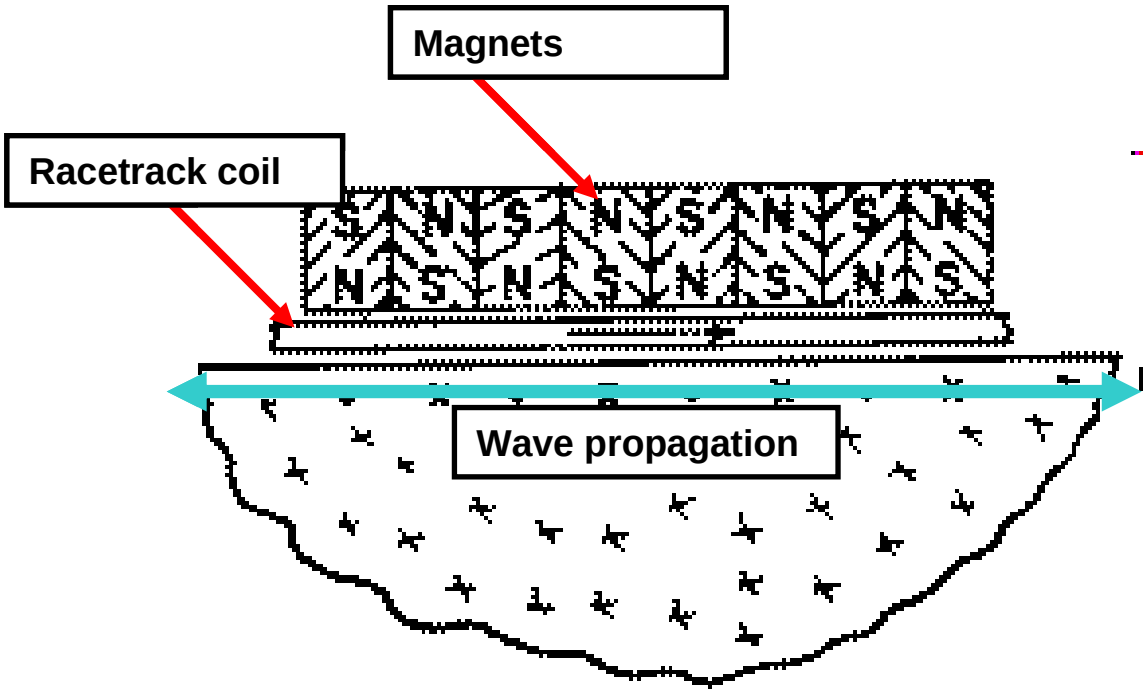

Figure 1.3 EMAT sensor diagram. [www.ndt-ed.org]

The EMAT works on the principle that when a current carrying wire is placed near an electrically conducting object and it is driven at the desired frequency, eddy currents are induced near the surface region of the object. When a static magnetic field is also present the eddy currents experience Lorentz force of the form:

F = J X B [www.ndt-ed.org, 2010].

The EMAT sensor is used widely in manufacturing environments where the material to be inspected is actually moving. The reason for this is that the sensors are relatively inexpensive and do not have to make contact with the material. So in the case of a field solution, and a sensor becomes inoperable, it can be replaced at little cost involved.

In order to detect longitudinal anomalies, through transmission sensors were placed in such a position that energy traveled longitudinally down the pipe as depicted in Figure 1.4. To detect circumferential direction anomalies, through transmission sensors were placed to send energy around the pipe circumferentially as shown in Figure 1.3.

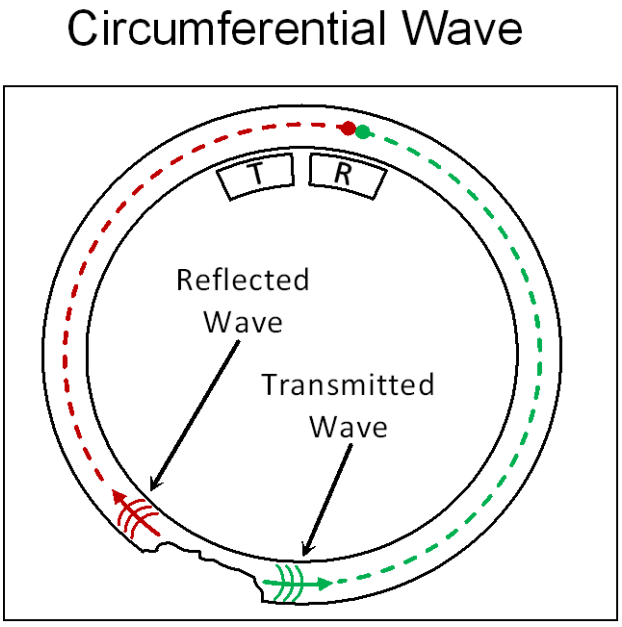

Figure 1.4 Circumferential travel direction of energy concept. [FBS Inc., 2010]

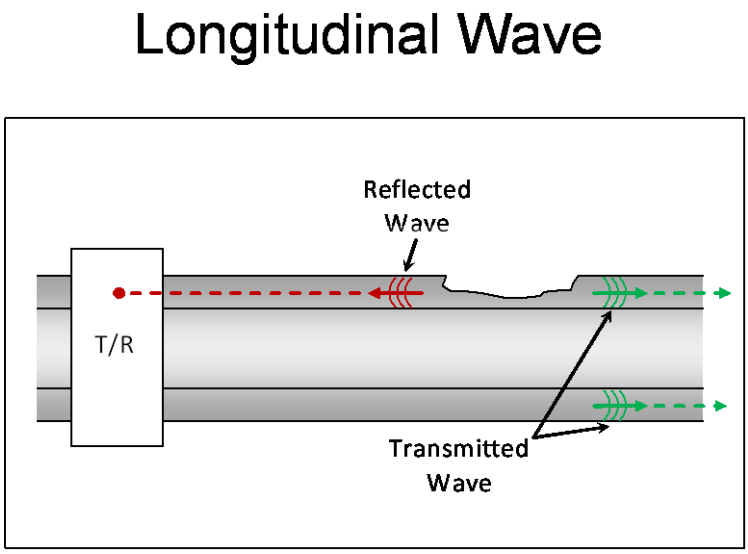

Figure 1.5 Longitudinal travel direction of energy. [FBS Inc., 2010]

Using this robust type of setup ensured that anomaly detection capabilities were high. A crack in any direction, along with corrosion, will be detected. Based on the sensor configuration that detects a defect, one can classify the type and/or approximate size of the defect. An encoder will be used to record tool position. A longitudinal direction crack would be seen by a pair of circumferential direction transducers. A circumferential direction crack would be detected by the longitudinal direction transducers. Using the data collected from the different transducers for different positions, anomaly length and type can be determined.

Chapter 2

FEASIBILITY STUDIES

2.1 Background

2.1.1 Deep Gas Well Storage inspection

The first step in the design of the final prototype sensor design was to optimize EMAT sensors. EMAT sensors were selected because of non-contact, no couplant required and ease of wave generation into a pipeline. The goal of the final tool is to use circumferential and axial oriented guided waves. The idea is to have guided waves being analyzed from the different configurations to help classify anomalies. A cluster defect pictured in Figure 2.1 was used in data collection with both types of set ups.

Figure 2.1 Machined cluster defect on the outside of a 4" schedule 40 steel pipe.

Various magnets with different thicknesses were used, as well as curved and flat magnets. Magnet thickness corresponds to wavelength; this allowed activation of different SH

modes with the different frequencies. Different size and shape magnets used are shown in Figure 2.2. The wavelength was set for the EMAT. This allows one to choose the desired mode by using the chosen wavelength to excite a certain frequency.

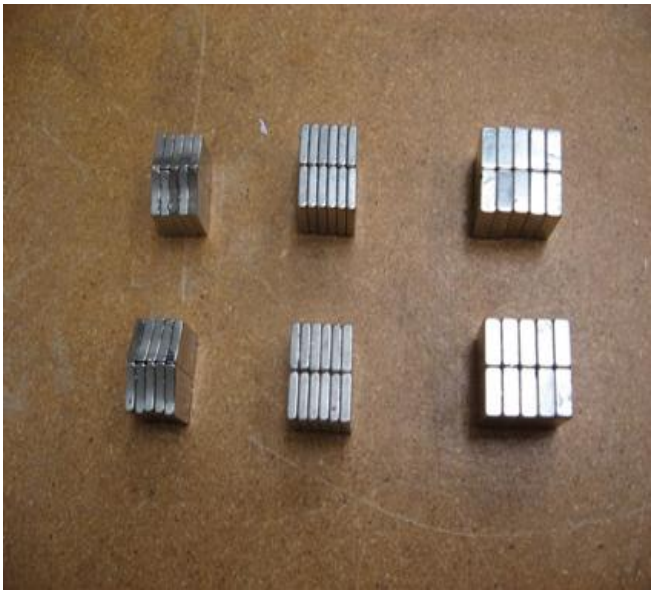

Figure 2.2 Various sized magnets used to generate different modes. Note the magnet thickness is what changes the wavelength.

2.1.2 Gas Distribution Line

Corrosion pitting is a problem in natural gas distribution pipelines. It often occurs in straight lines along the pipe axis with multiple pits when present, as seen in Figure 2.3. The defects take on a circular or elongated circular shape. Internal pitting corrosion, caused by carbon dioxide (CO_2) and hydrogen sulfide (H_2S), is one of the predominant failure mechanisms of these pipelines. [Papavinasam S., 1999]

Figure 2.3 A photo of pitting corrosion along the axial length of a 12" pipe that was taken out of service.

A meander type EMAT was chosen to tackle axial corrosion pitting because of its unique characteristic of generating Lamb type waves in the pipe. It works on the principal that Lorentz forces are generated when a wire is placed near the surface with a static magnetic field. A coil was chosen based on the desired mode generation. The spacing between coil windings with current flowing in one direction determines the wavelength. If a straight line is placed on the

dispersion curve with a slope of the wavelength, then it is possible to excite all modes that cross the line. A meander type EMAT set up can be seen in Figure 2.4.

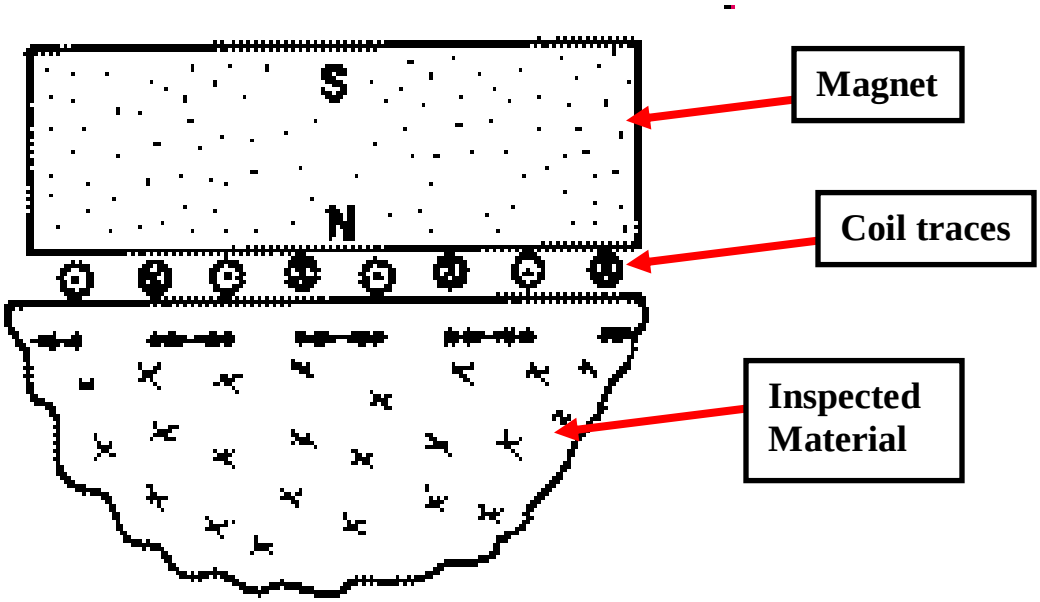

Figure 2.4 A meander type EMAT set up with a magnet on top of an alternating direction current coil between the sample inspected and the magnet [www.ndt-ed.org, 2010].

For the experiments performed to detect corrosion pits, two different EMAT setups were used. A pulse echo design was used to detect a reflection from the simulated corrosion. A through transmission design was used to detect an amplitude drop in the received signal. This drop in amplitude is due to interference around the simulated corrosion.

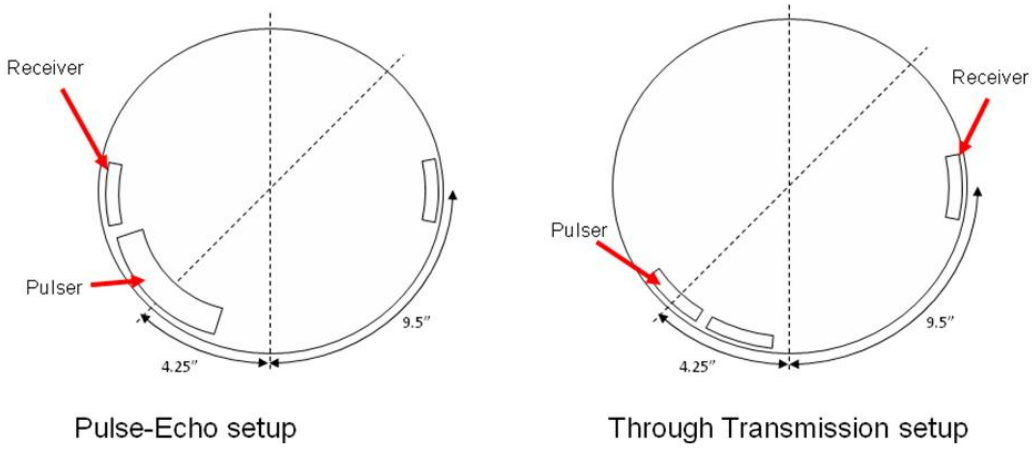

Figure 2.5 A drawing showing the sensor placement for pulse-echo and through transmission is shown above.

In either set up a geometrically focused coil was used to focus the energy at a point where the suspected corrosion would be found. This promotes the ability pinpoint the region of the pipe that is of interest.

The through transmission setup was designed to detect an amplitude loss in the through pulse as energy is lost or scattered around a defect. The pulse-echo setup shows reflections from the defects.

2.2 Frequency and mode selection

2.2.1 Deep Gas Storage Well

Different modes and points along the dispersion curve, generated by FBS Inc. and shown in Figure 2.6, were chosen. Then after experiments using all modes of interest, the one most sensitive to defect detection through experimental selection was chosen.

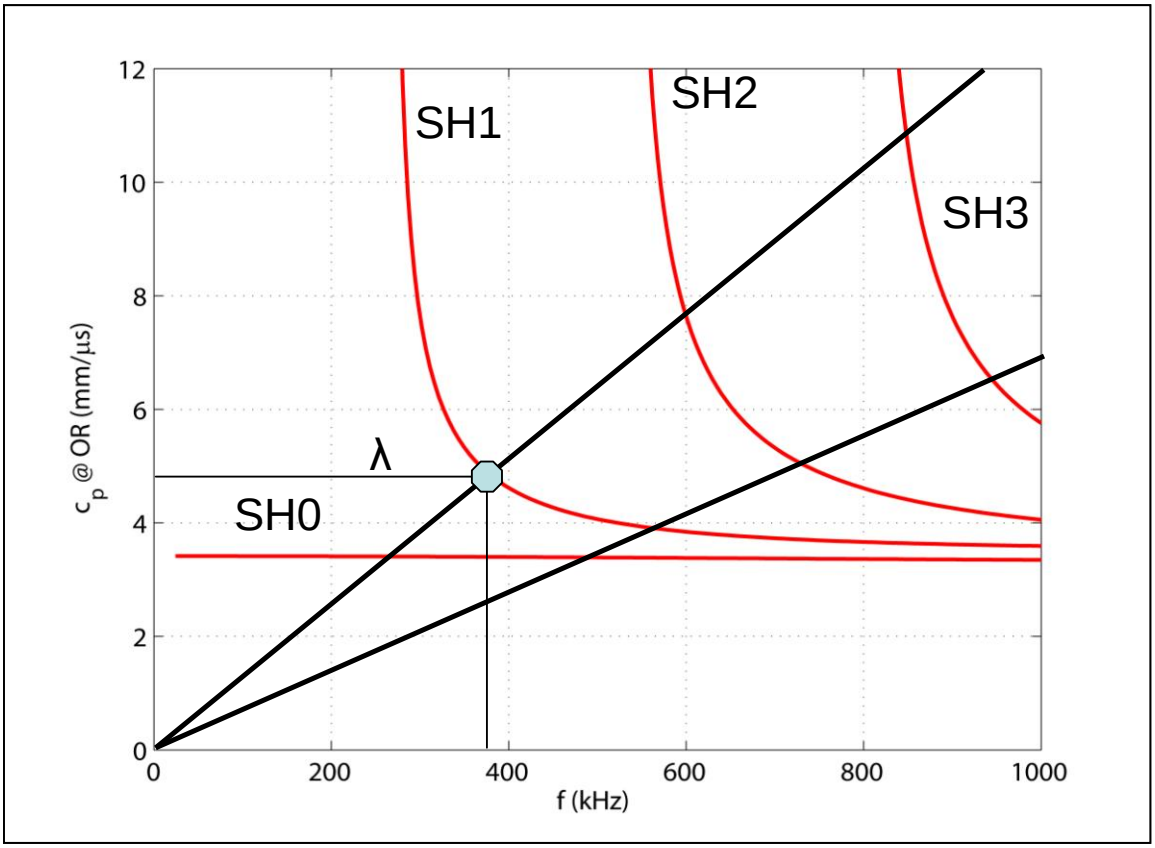

Figure 2.6 A sample dispersion curve for shear horizontal guided waves showing slope activation concept for an EMAT. [FBS Inc., 2010]

Analysis of the dispersion curves leads to making educated decisions on what frequencies should be best for defect detection. The SH0 mode is non dispersive, which means that the speed of the mode is not frequency dependent. This is a desirable trait to have because this should avoid mode conversion if the frequency used is below the first cutoff frequency of SH1, around 300 kHz, and little mode conversion beyond 300 kHz. To pick the point you want to use on the dispersion curve, a mode and speed must be chosen. The type of EMAT used was a periodic permanent magnet EMAT. The complete sensor consists of a racetrack coil placed near the surface and the magnets placed on top on the coil. The slope of the activation line is determined by the magnet thickness.

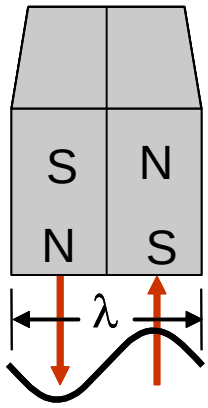

Figure 2.7 A graphic depicting how wavelength is determined based on magnet thickness. [FBS Inc., 2010]

The slope of the curve is the wavelength that can be generated with the specific magnets being used. As can be seen in Figure 2.7 the thickness of two magnets is the wavelength.

2.2.2 Gas Distribution Line

The experiments conducted in this study used different modes in detecting and determining the depth of defects. Originally the asymmetric mode A0 was used on machined elongated defects. Later the discovery was made that this mode was not sensitive to circular defects. Both types of defects are shown in Figure 2.8.

Figure 2.8 To the left is a picture of a 30% through wall circular defect. On the right is a 50% through wall elongated defect.

This discovery was found when trying to locate circular pitting defects on an out of service pipe with real corrosion. Different modes were checked along the dispersion curve as shown in Figure 2.9 and the symmetric S1 mode was chosen based experimentally on its sensitivity to real corrosion defects. For the meander type EMAT chosen the slope of the black line in Figure 2.9 is the wavelength, this can be adjusted by moving your coil spacing either closer or farther apart. The meander type EMAT is used to generate a longitudinal guided wave. All experiments were limited to the slope shown because the type of coil manufacturing used was expensive and time consuming. Being able to change the slope would allow the activation of the same modes at different frequencies.

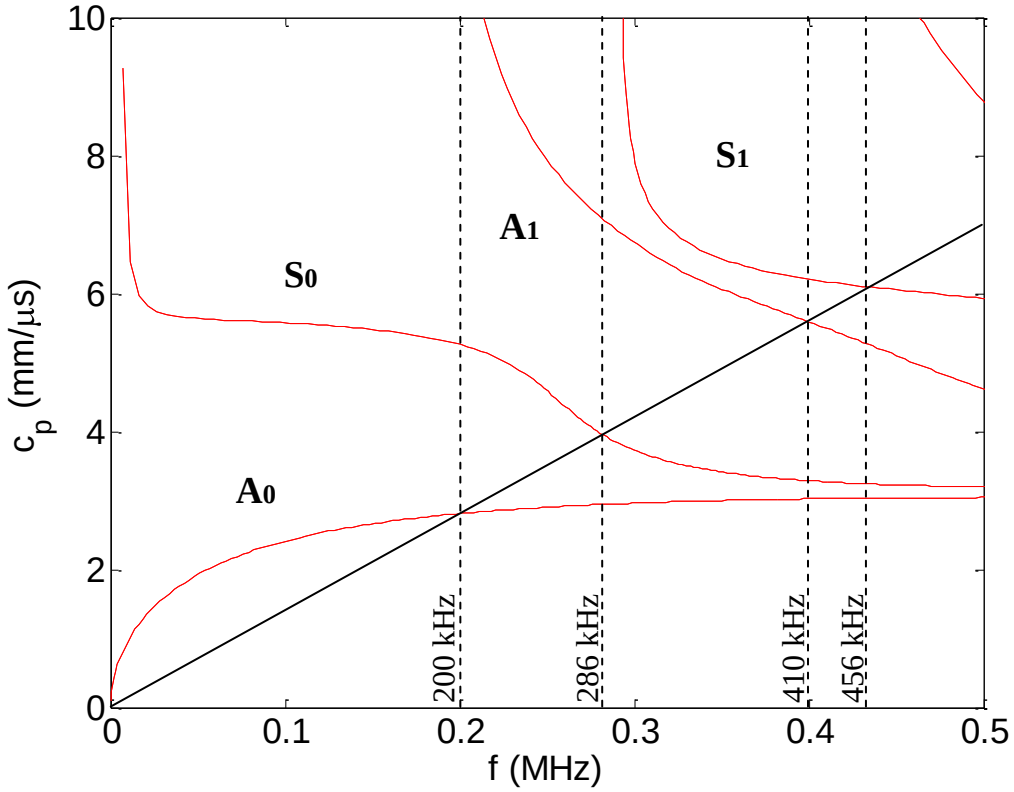

Figure 2.9 A phase velocity dispersion curve for Lamb type waves in a 12" schedule 40 pipe [FBS Inc., 2010].

The A0 mode proved to be sensitive to the elongated defects but not to perfectly round holes which more accurately represents real world corrosion. The S1 mode generates an efficient guided wave that detects real corrosion with little mode conversion. An example of defect detection is seen in Figure 2.10.

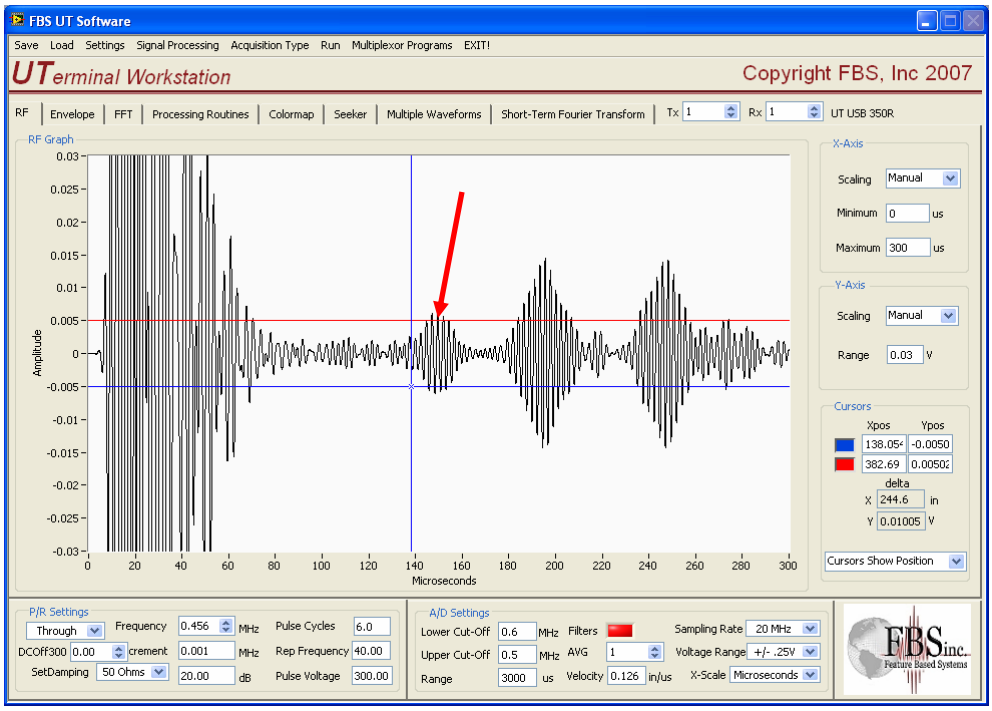

Figure 2.10 A reflection shown from a circular corrosion defect at 140μs using the S1 mode

Chapter 3

EXPERIMENTAL RESULTS

After all sensor design and details were chosen for the inspection of a gas storage well, and gas distribution line; experimental verifications of the chosen sensors was needed. Defect detection and sensor optimization was verified. This ensured the best sensor choices were made before the construction of prototype tools to be used inside of pipes.

For the gas storage well inspection tool, both circumferential direction and longitudinal direction sensor setups were used simultaneously. In the case of the gas distribution line inspection tool, circumferential direction guided wave sensors were employed.

For both tools the correct mode and frequency were chosen based experimentally on defect sensitivity.

3.1 Circumferential Direction Gas Storage Well

Data was collected at 475 kHz in the circumferential direction around a clean section of 4- inch schedule 40 carbon steel pipe with a cluster defect that was previously shown earlier in Figure 2.1.

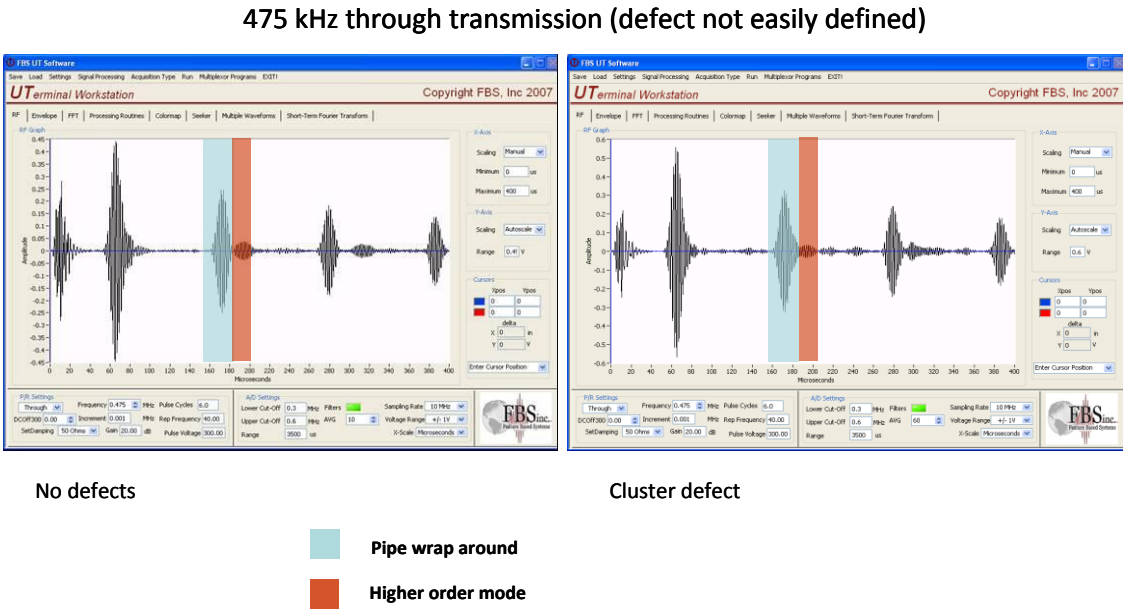

Figure 3.1 Experimental results at 475 kHz on a section with and without cluster defects are shown.

In Figure 3.1 there is no clear reflection from the defect. Results show that there was a higher order mode present at this frequency. This made defect detection difficult. Much better results were obtained when the 280 kHz frequency that excited the SH0 mode was used. Results are shown in Figure 3.2. At this lower frequency, no higher order mode is present, Using the SH0 mode, defect detection was more reliable, and false calls were eliminated.

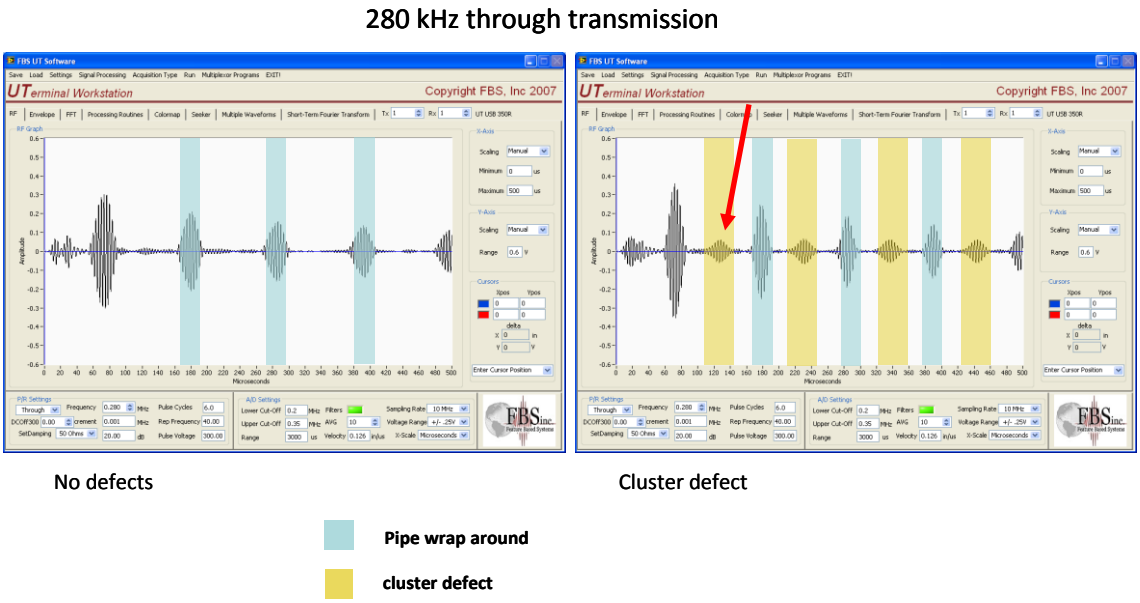

Figure 3.2 Experimental results at 280 kHz on a section with and without cluster defects are shown.

Further verification of the SH0 mode at 280 kHz being superior was needed. As one can see in Figure 3.2, a cluster defect was detected very readily with no mode conversion and very little noise. A comparison of the SH1 mode was made at 362 kHz for defect detection.

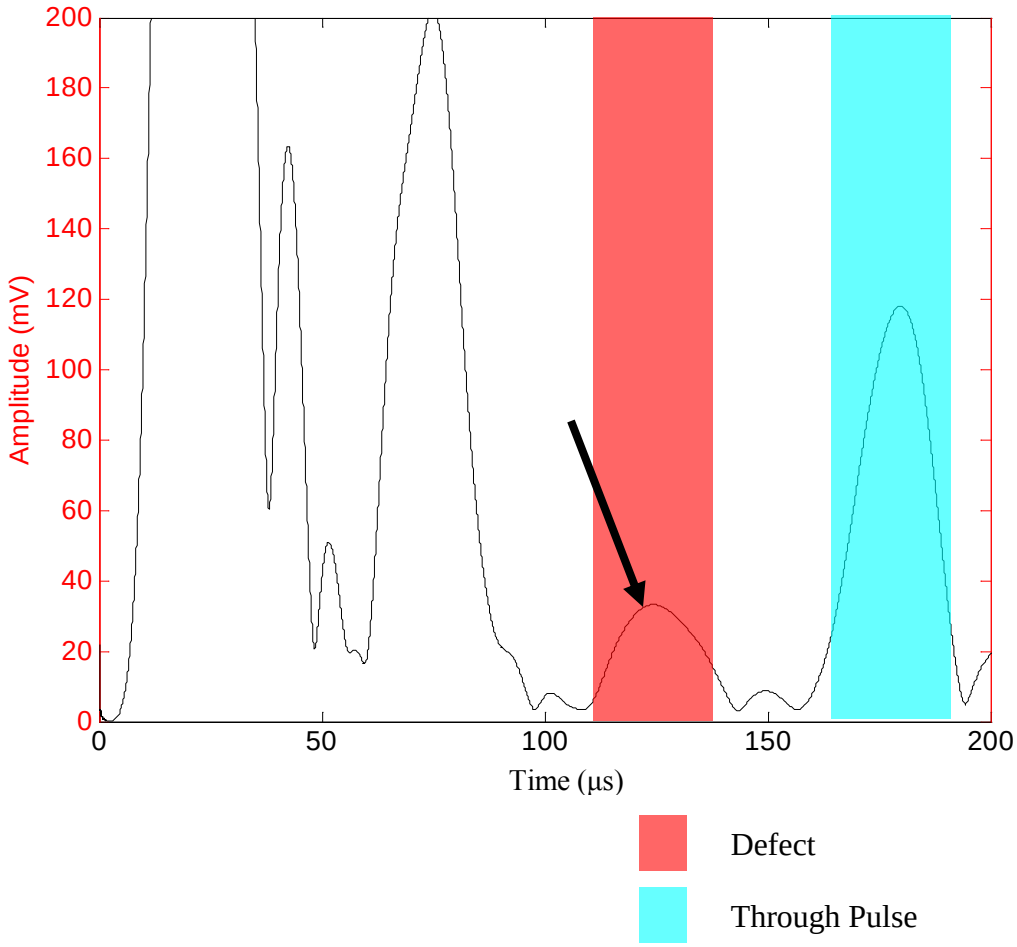

Figure 3.3 Defect detection at 270 kHz with the SH0 mode.

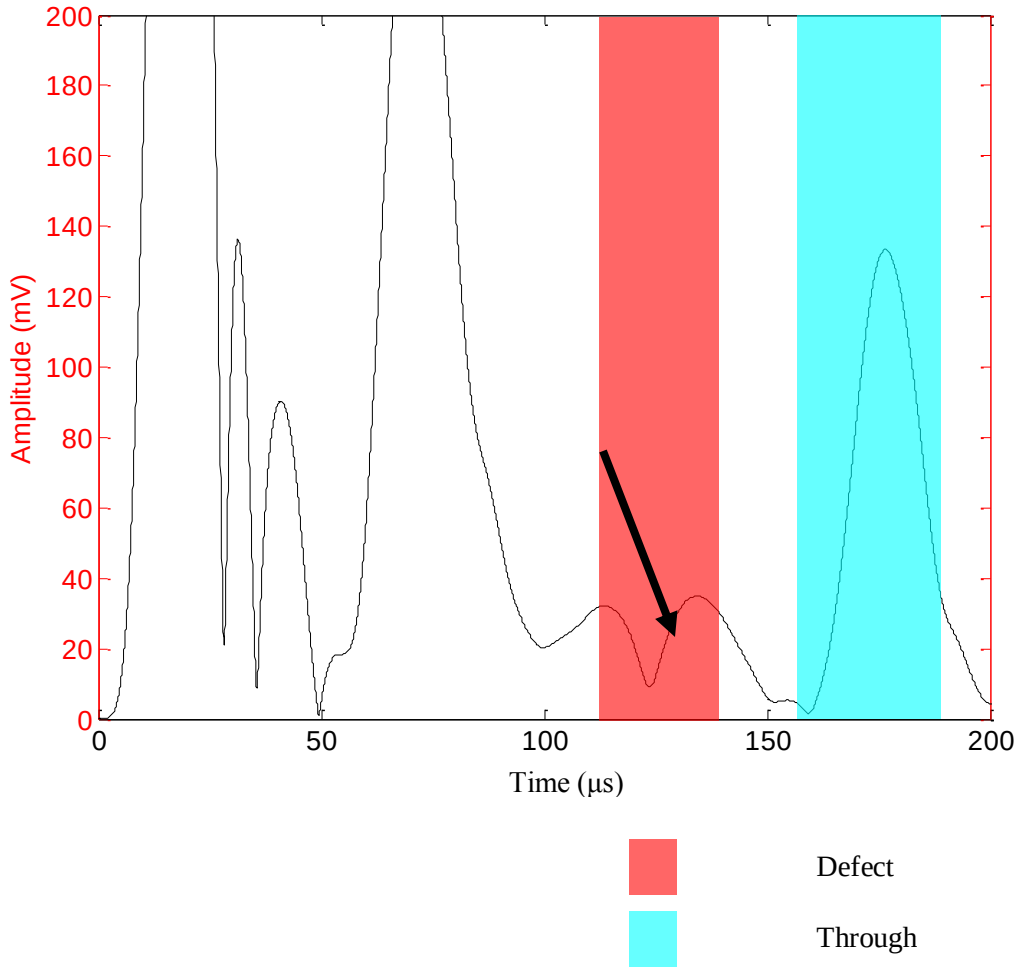

Figure 3.4 Defect detection at 362 kHz using the SH1 mode.

From the above two figures 3.3 and 3.4 one can see that superior defect detection is seen at 270 kHz using the SH0 mode. When using the SH1 mode at 362 kHz there is mode conversion at the defect. This mode conversion could prove troublesome with defect detection reliability. The SH0 mode once again has a lower noise floor and a very clear defect reflection at 125μs.

3.2 Circumferential direction gas distribution line

Being able to focus energy at the bottom of a gas distribution line was paramount for the defects of interest. This enables the classification of the worst kind of defects, which is pitting at the bottom in a line. Different sensor and coil configurations were used to determine the best approach. A single straight coil, single curved coil, and a large geometric focused array were used.

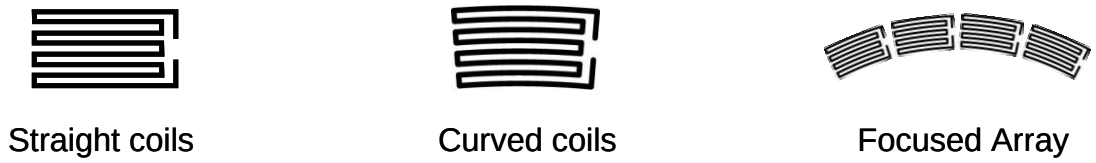

Figure 3.5 Coil configuration drawings. [FBS Inc]

Each of the coils were placed on a 0.243" thick steel plate with a 1 inch by 0.5 inch long machined corrosion with a depth of 0.122". The A0 mode was pulsed at 200 kHz in a through transmission experiment while receiving with a single straight coil. The pulser coil types from Figure 3.5 were the variable of experimental results shown in Figure 3.6.

a)

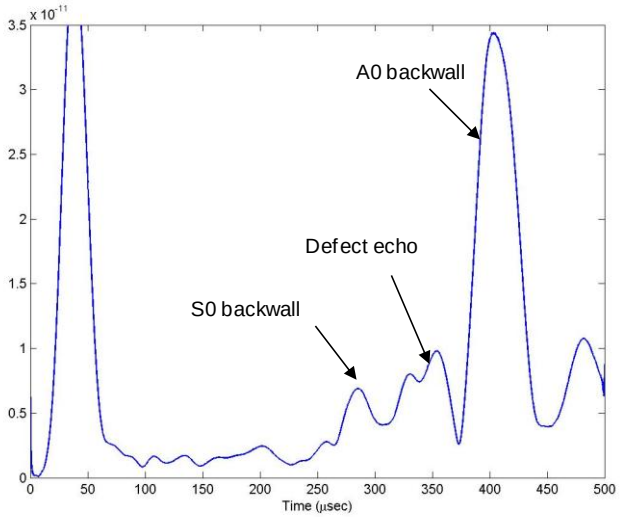

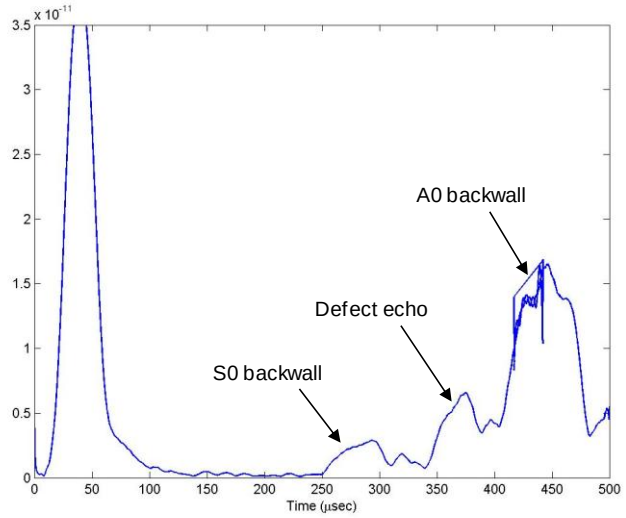

b)

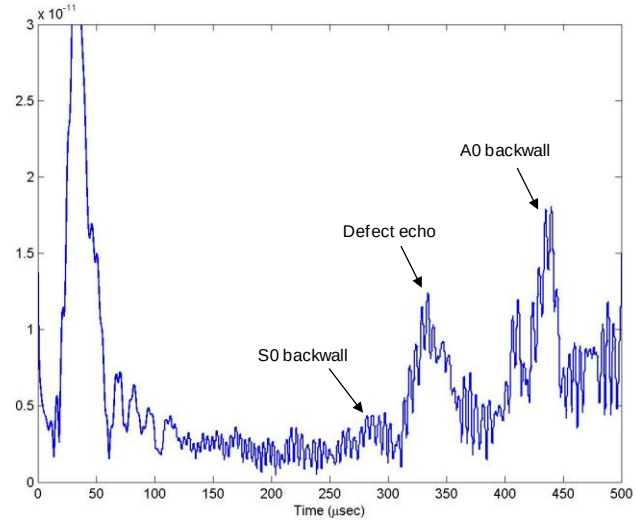

c)

Figure 3.6 Waveforms from different pulsing coils; a) straight coil, b) single curved coil, c) geometrically focused coil. [FBS Inc., 2010]

When the ratio of the defect echo and the A0 backwall was taken, the large geometrically focused array had the highest ratio. This meant that more energy was being focused at the defect with this setup, and therefore more energy was being reflected, which is what was expected.

3.3 Longitudinal Direction gas storage well

The longitudinal directional sensors must also be verified to work well with the same frequency as the circumferential sensors. A prototype tool is limited to using one frequency at once for both set ups. A cluster defect is best defined using, the SH0 mode at 280 kHz. Therefore, this mode must be verified with the longitudinal direction setup and results are shown in Figure 3.7 and Figure 3.8.

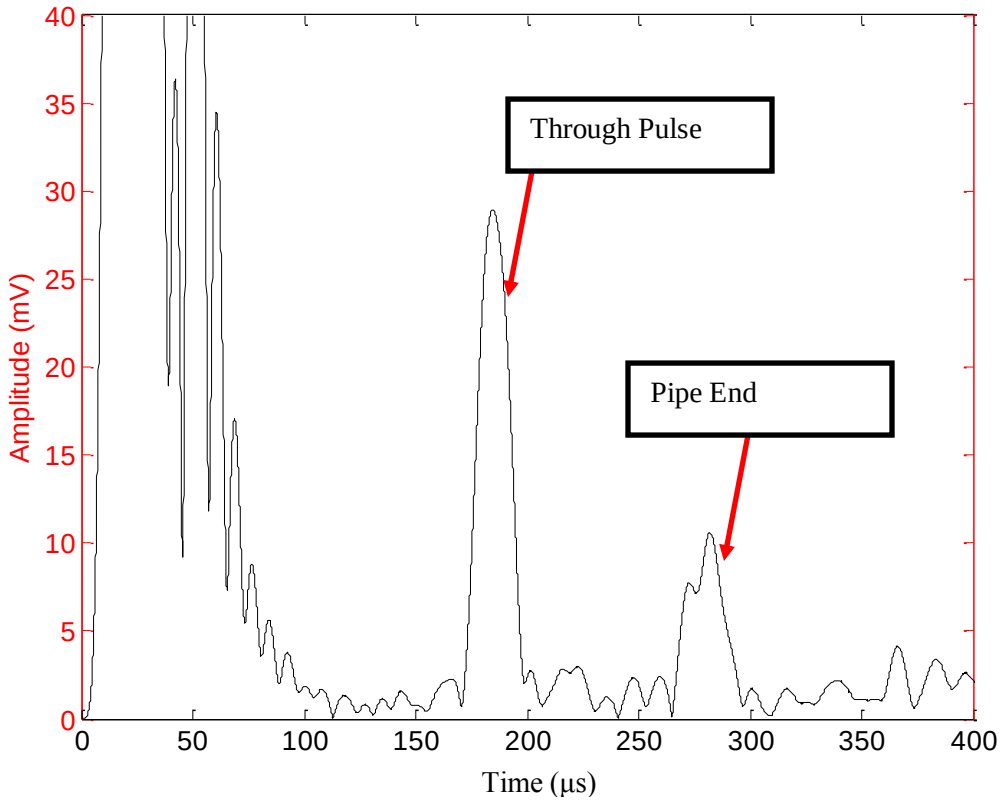

Figure 3.7 Longitudinal direction sensor results at 270 kHz. Notice the through pulse at 175 μsec.

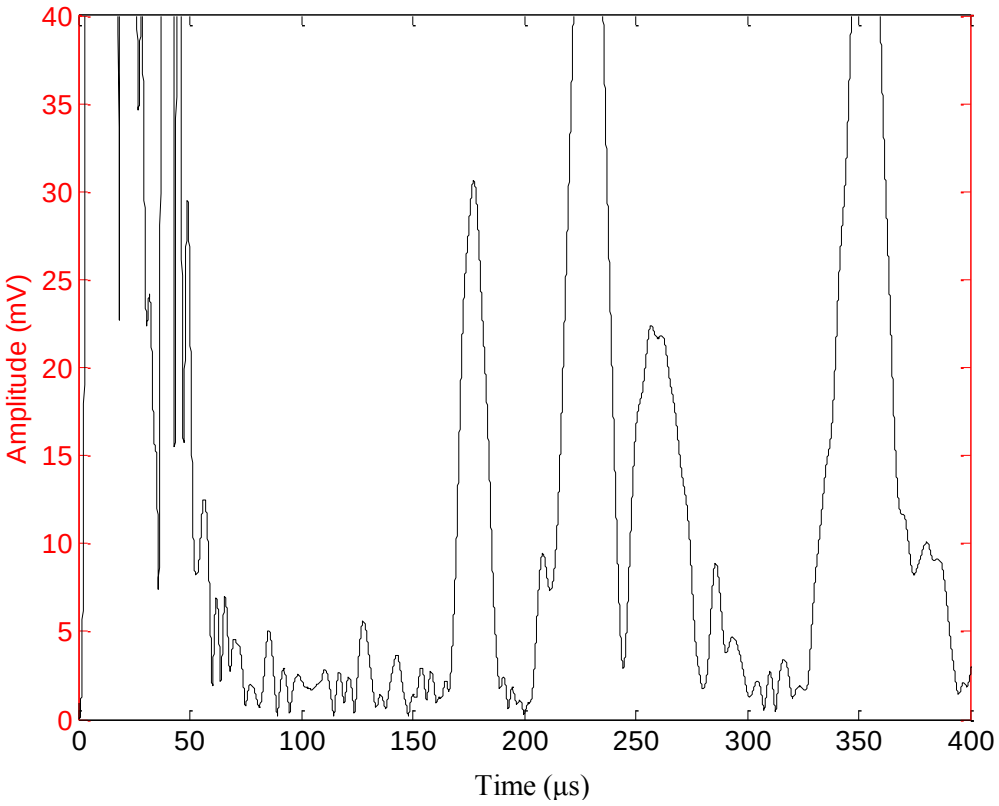

Figure 3.8 Longitudinal direction sensors at 362 kHz.

After the longitudinal sensors were run at different frequencies to excite different modes, it was clear that once again the SH0 mode was a superior mode to use. The noise is much lower from the initial pulse to the pulse being received. Also, one can see in Figure 3.8 that there are other modes coming in after the initial pulse, this behavior will lead to noise and defect detection problems. In the event of anomaly detection, this could lead to confusion if there would be some possible mode conversion, noise, or indeed a defect.

3.4 Gas Storage Well Interference Experiment

One concern that was raised was that once both circumferential and longitudinal setups were used together simultaneously; there would be the possibility of wave interference. Both directional sensor setups would have to be pulsed and received simultaneously due to only having one pulse amplifier. First, the longitudinal direction sensors were set up and tested. Shown in Figure 3.9 is the longitudinal setup pulsed alone on a section of clean pipe.

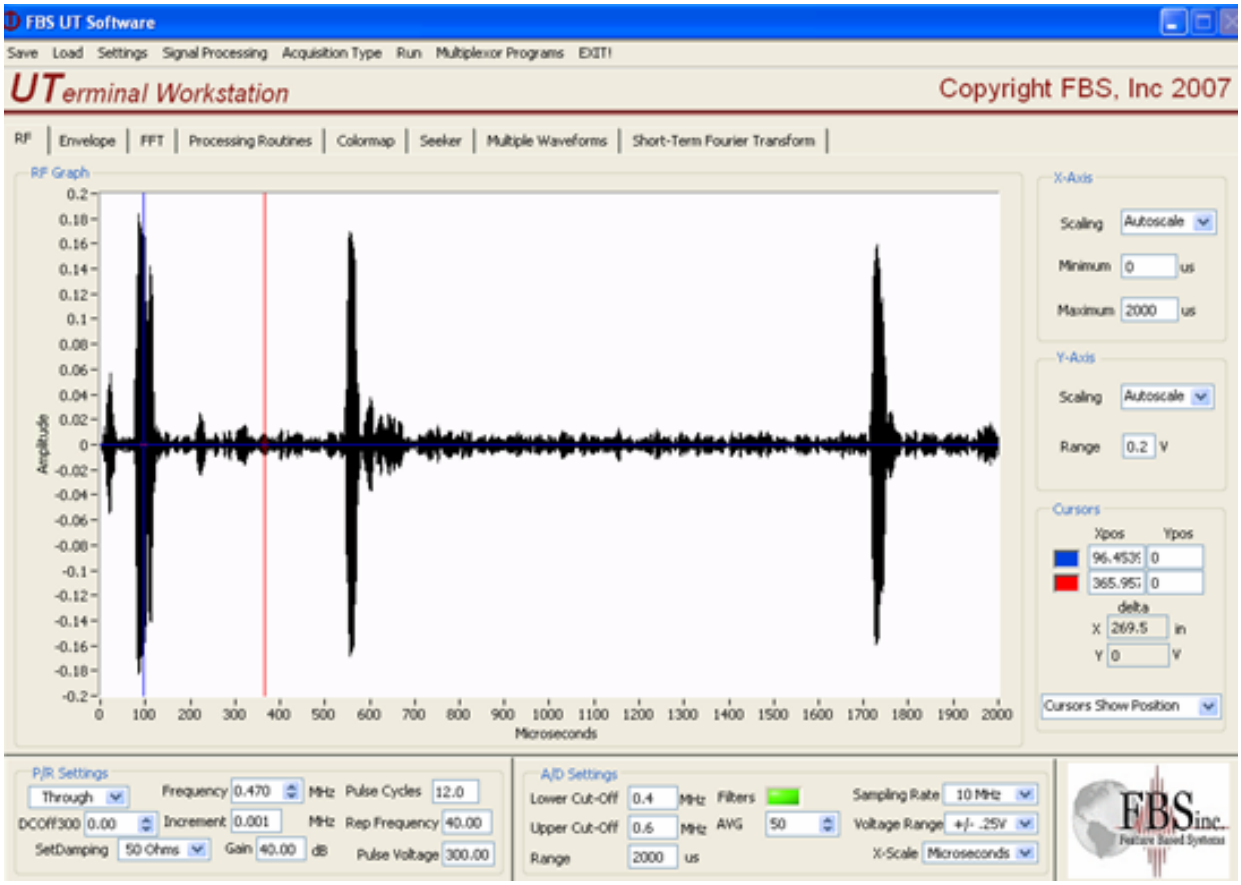

Figure 3.9 Longitudinal setup pulsed alone on a section of clean pipe. [FBS Inc., 2010]

The longitudinal interference comparison was done at 470 kHz. This reiterates the fact that frequency is not optimal because of noise present in Figure 3.9, but proves there is no

interference when using both setups at the same instant. This experiment was done before the manufacturing of the curved magnets made of the thickness to activate the SH0 mode at 270 kHz were completed. A signal with the longitudinal setup is affected at the main bang when both setups were pulsed simultaneously as can be seen in Figure 3.10 compared to Figure 3.9. The main bang is the initial pulse, and usually an unusable part of the signal for the first few hundred microseconds. However, the signal is still very usable when the circumferential setup is pulsed at the same time.

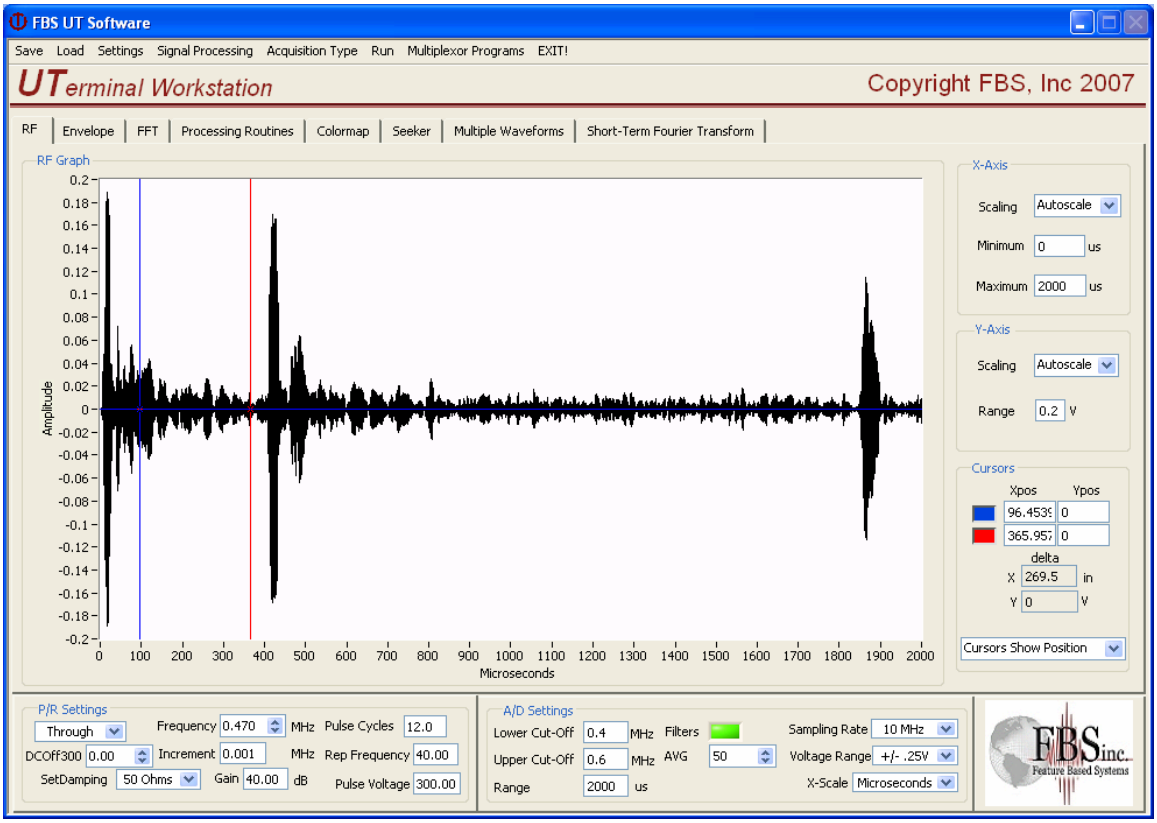

Figure 3.10 Longitudinal setup received while pulsing a circumferential setup on the same pipe. [FBS Inc., 2010]

The circumferential setup experiment also produced acceptable results. The only difference when pulsed simultaneously with the longitudinal set up was an amplitude loss shown in Figure 3.11 and Figure 3.12. This was expected and is due to the energy being sent to more

than one pulser. Once all three transmitters were connected to the amplifier the energy output to each is dropped.

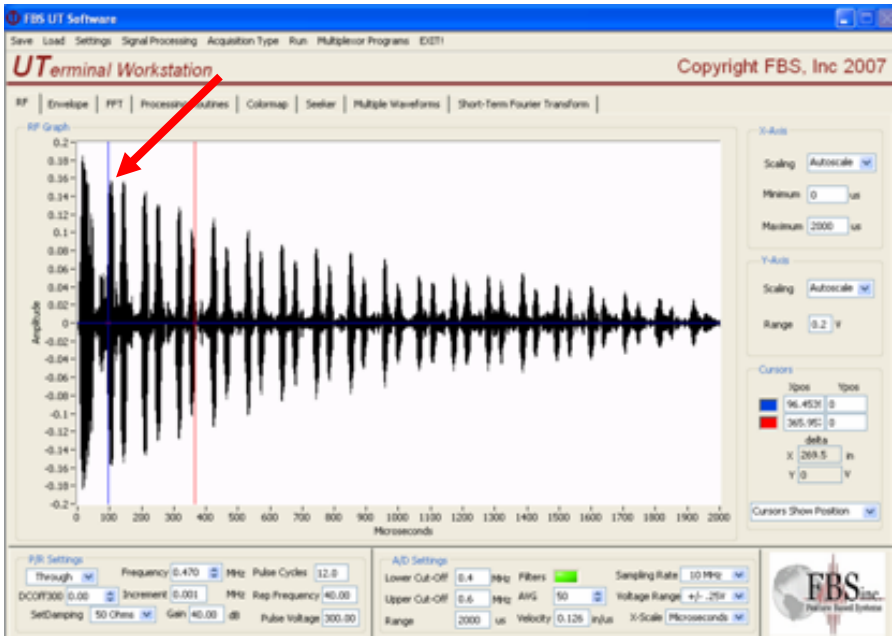

Figure 3.11 Circumferential setup pulsed and received alone. Note first wrap around signal amplitude at about 0.16 V. [FBS Inc., 2010]

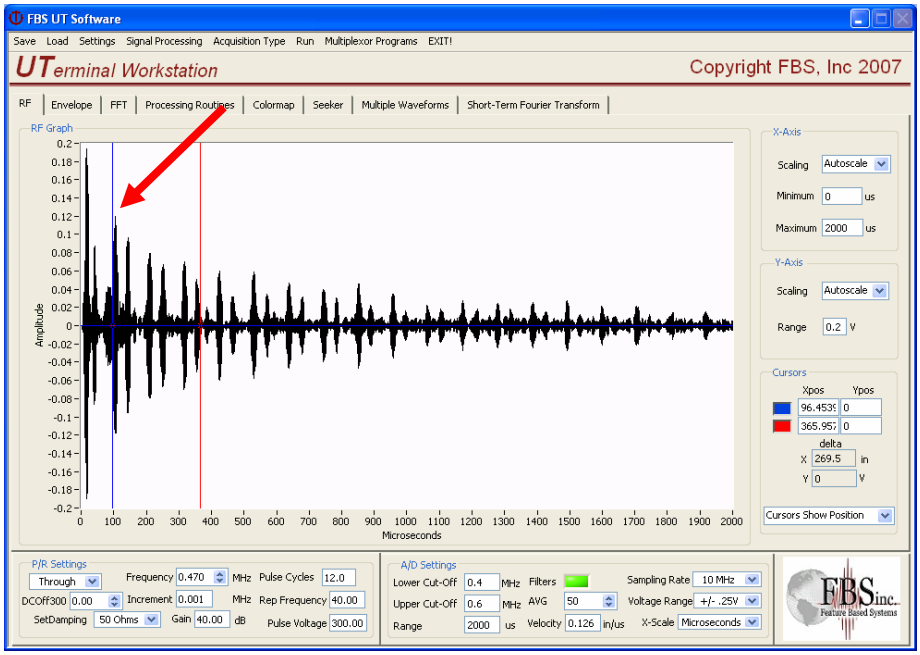

Figure 3.12 Circumferential setup pulsed and received with longitudinal set up being pulsed. Note first wrap around signal amplitude at about 0.12 V. [FBS Inc., 2010]

To be sure there was no wave interference, one last precautionary experiment was performed. The longitudinal pulser was moved to another pipe while still pulsing and receiving with the circumferential setup, the signal after this is shown in Figure 3.13. The signal is not affected once this is done and the amplitude is still lower. This proves the amplitude drop is only due to pulser energy distribution.

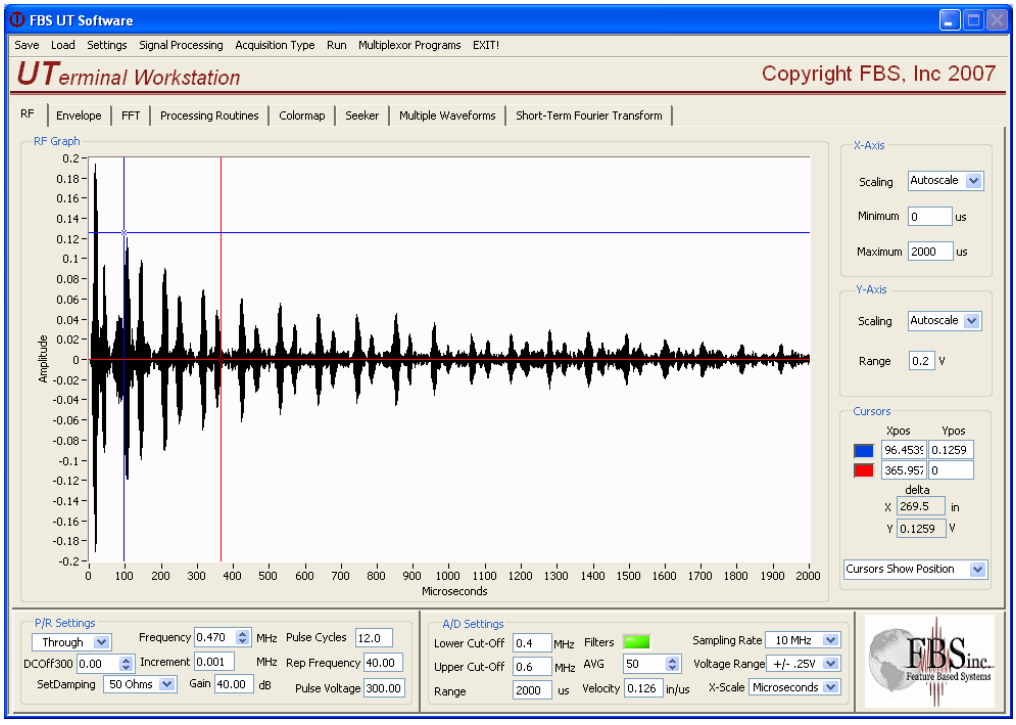

Figure 3.13 Circumferential signal received while the longitudinal setup is moved to another pipe.

Hundreds of experiments were performed altogether with different circumferential and longitudinal transducers. They showed that there should be no complications once mounted together in a prototype tool. These initial experiments were necessary to ensure no wave interference. The pulser and receiver distances and setups were all taken into account in the final prototype design.

3.5 Sensor Selection Conclusions

Six sensors were tested experimentally and one was clearly identified as the better choice for defect detection in a gas storage well. The main attributes needed are a low noise floor, no mode conversion, and clear defect detection. Different modes with different wavelengths were all tested.

For the circumferential direction, a wavelength of 0.157 inches was chosen and the SH1 mode was excited at 456 kHz. This transducer set up showed mode conversion. Using a wavelength of 0.394 inches, the SH0 and SH1 mode were both excited using different frequencies. The SH0 mode was excited at 270 kHz and 280 kHz, while the SH1 mode was excited at 362 kHz. The different excitation frequencies for the SH0 mode were not done for any specific reason. The 10 kHz frequency difference was between different experiments and had no direct impact on the results that was observed. The same trends were observed at both frequencies.

Again at the longer wavelength the SH1 mode had mode conversion and a higher noise floor. The higher noise floor is believed to be a result of the higher order mode presence.

Longitudinal direction sensors were experimentally verified at the 0.394 inch wavelength and showed the same trends as the circumferential setup with this wavelength. The low noise floor of the SH0 mode is needed to eliminate false calls.

Both circumferential and longitudinal direction setups were verified to be at optimal working condition using the SH0 mode at 270 kHz. The defect detection and verification for this configuration is straightforward due to the non-dispersive nature of the mode.

In the gas distribution line a geometric focused array coil was chosen to concentrate the energy in potential defect areas. The S1 mode is most sensitive to real corrosion defects and will be incorporated in the final prototype.

Chapter 4

PROTOTYPE DESIGN

4.1 Key component selection

4.1.1 Coil protection

The environment that the tool will operate at inside of a gas storage well or distribution line is known to be harsh. Storage wells that have been in use for an extended period of time are considered to be an accelerated corrosion environment. This will cause the steel casing to be a corroded rough surface with scaling. A sensor can not just be simply the coil used in lab experiments. This would put the coil in contact with a surface having the potential to tear the traces. As previously mentioned, the coil does not have to be in direct contact with the casing. A urethane material was used to protect coil traces. Urethane material had proved successful in coil protection as seen in Figure 4.1.

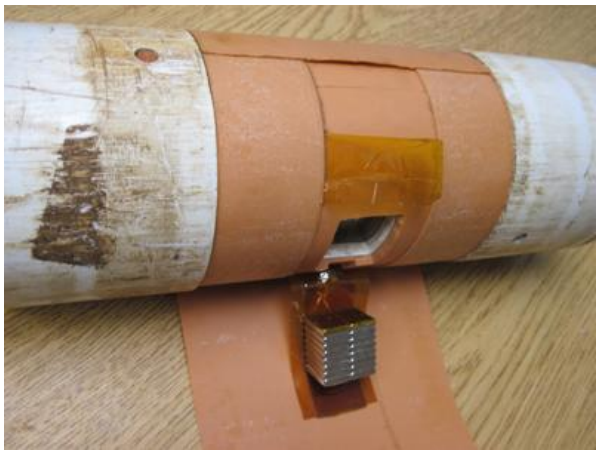

Figure 4.1 A previous gas storage well project design used a urethane sheet to protect the coil traces. [Parayitham, 2008]

4.1.2 Tool position tracking

The next obstacle is that the tool position needs to be tracked in the well casing. An encoder was used to perform this task. The idle storage well that the tool was used for testing was known to have water and moisture content. After being idle the well had filled with water. The tool was not expected to be completely submerged in water. An environmentally sealed package was chosen to be incorporated into the design. A very small encoder is needed to be able to fit into the 4 inch pipe and be housed inside the tool, the gas storage well encoder is shown in Figure 4.2. Although the gas distribution line tool does not have the same size limitations, the encoder should be rated for harsh environments.

Figure 4.2 A off the shelf encoder to IP65 specification that is spring loaded.

A spring loaded mechanism was built into the encoders that will be used to ensure that the wheel is in contact with the pipe at all times. This strong contact with the pipe wall was crucial to ensure correct tool position registration down the well, or in a line. If position registration is lost, all data collected would be compromised.

4.1.3 Robust and interchangeable coil

The racetrack coil used also needed to be mounted securely to the tool. Initial experiments were done with simple Mylar coated copper traces.

Figure 4.3 A bare bones EMAT sensor set up. Magnets are placed directly on a racetrack coil.

The manufacturer who makes the basic coil design also manufactures a similar design coil with mounting holes for a circular push-pull connector. The circular connector is shown in Figure 4.4. Modifications were made to the coil layout and connector placement, and then design was manufactured to my specifications to accommodate both the circumferential and longitudinal head designs. This proved to be a robust design and allowed for ease of removal and coil replacement in the event of coil failure. If mounting points were not used in the coil placement over the magnets, this would compromise magnet positioning over the coil, and the ultrasonic energy transmitted into the well casing would not be maximized. This circular connector was a specification that also addressed issues with coils tearing at solder pads and having free hanging wires. In the center of Figure 4.3 one can see the solder pads and wires. With many sensors loose

wires create a mess, and are undesirable. Imagine this moving through a well casing at 5 mph and becoming snagged on a piece of corrosion scale.

Figure 4.4 An off the shelf EMAT coil design with a board mount circular connector and mounting holes.

4.1.4 Pre-amplifier

The initial pre-amplifier solution was to purchase an off the shelf unit. This was unsuccessful due to the cost of redesign to house the electronics inside a 3” diameter envelope. A pre-amplifier board circuit designed by FBS Inc. was used. The small existing design was repackaged to have BNC and circular Lemo connectors. The pre-amp was mounted inside a small aluminum enclosure that was then mounted inside the tool.

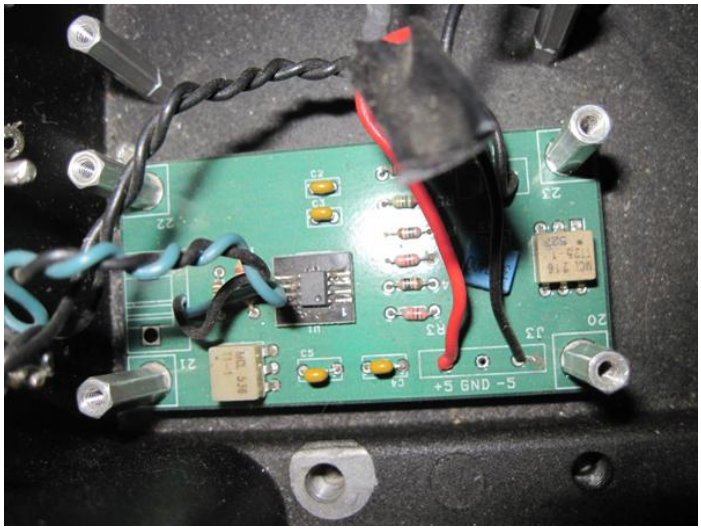

Figure 4.5 A previously designed pre-amp that was repackaged to be used with the electronics, coils, and fit inside the well casing integrity analysis tool.

4.2 Gas storage well tool design

4.2.1 Initial gas storage well tool concept

Previous work had been done to assess the potential of using circumferential guided waves in a gas storage well. The first prototype was used as a feasibility test of circumferential direction EMATs inside a 4 inch schedule 40 carbon steel pipe. There were a few issues with the original prototype that had to be addressed. If there were pipe inner diameter size inconsistencies the tool would not fit. The tool was permanently sized to fit just inside a 4 inch schedule 40 pipe. Additionally, at the well head the different fittings and flanges posed a problem in having the tool fit down the well. Knowing these issues and taking them into account, the decision was to make a tool that would have a 1 inch tolerance below and above a 4 inch schedule 40 pipe inside diameter. A prototype that utilized axial and circumferential waves was designed. To aid in the initial design stage, a needs matrix was constructed, and is shown in Table 4.1.

Table 4.1 Design needs matrix for a gas storage well case integrity inspection tool.

Need \ Metric	1" diameter variability	Circumferential waves	Axial waves	Coil surface protection	EMAT to pipe Contact minimized	Minimize electronics housed in tool	Tool encasement	Pneumatic operation	suspension	Aluminum construction	Facilitate waterjet capabilities
Variable pipe size	X										
Detect corrosion		X	X								
Detect axial defects		X									
Detect longitudinal defects			X								
Indentify loose joints			X								
Robust				X	X	X	X	X			
Home position must be retracted								X			
Tool always centered									X		
lightweight										X	
Reliable data collection				X	X			X			
prototype cost effective											X

A spring loaded waterproof and dustproof packaged encoder was to be used in the final design. This ensured accurate data collection as the tool was pulled through a well. An abrasion resistant urethane was used to protect the coil in the final design. It proved very robust when used in the initial prototype testing. A board mounted Lemo connector is currently being utilized on the EMAT coils. This is a nice feature and eliminates the need to solder directly to a solder pad on the coil. During testing the solder joint is often a point of failure for EMAT coils.

Basic desired operation of the tool is simple. The tool is lowered down into a gas storage well, and then once in place expanded outward to have the EMATs make contact. Finally the tool would be pulled up out of the well and take data continuously at predetermined increments. The

initial design phase was completed, then any components that could be improved upon were narrowed in on and corrected. The initial 3-D model and comments are shown in figure 4.6.

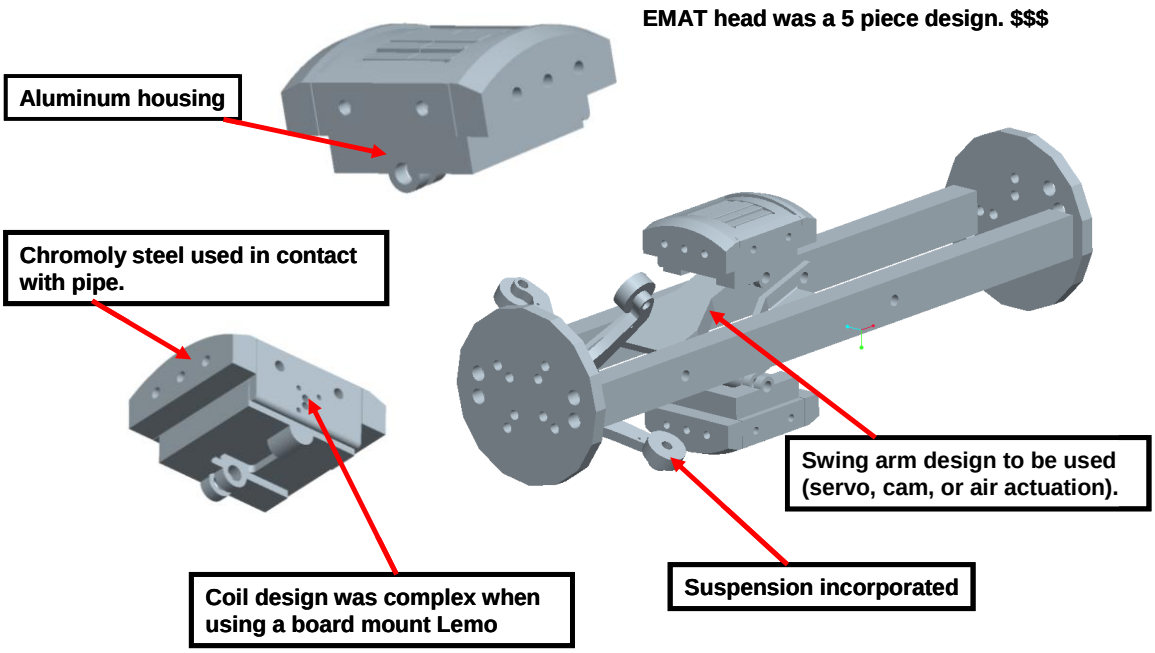

Figure 4.6 A 3-D cad design of the initial prototype tool that would be improved upon.

The initial prototype concept design was improved upon in many ways. Shown in Figure 4.6 is the first concept tool that was never manufactured. The EMAT housing was a five piece design. Chromoly was used as the wear surface to be in contact with the pipe. These pieces would bolt to the aluminum housing that would hold the magnets, coil, and urethane. This many pieces would be expensive to manufacture. The design was not easily adaptable to create axial aligned EMATs. In Figure 4.6, only the circumferential EMAT heads are shown. The coil design would be complicated and would not wrap nicely around the compound bends as needed in this first design phase. Due to the limited space swing arms were used from a different direction for each

EMAT head. This had the potential for the heads to be misaligned while taking data. A suspension was used to keep the tool centered in the pipe. In a perfect world the tool might have rode in the center of a pipe. The design had potential for over 0.25" misalignment. That is more than enough misalignment to produce unreliable results. Also, cam or servo actuation that was originally planned would have been a favorable way to actuate the EMAT heads. On the contrary if there were to be an electrical problem, the EMATs could be stuck in the outward position. If the sensor heads would become stuck in the well this would cause the tool to become permanently lodged in the casing. This is unacceptable and would cause major problems with the well if in use. With the correct type of air actuation, in the event of any malfunction, the EMATs would lose contact and return to the inward position. This can be accomplished using spring return air cylinders.

4.2.2 Final sensor head design

The final design of the EMAT heads utilized an air cylinder with a wedge that would push the two heads directly apart from each other. The two heads will ride in the same grove. This design consideration ensured that each head moves outward the same amount, and misalignment is not an issue because the tool will self center. As shown in Figure 4.7 springs are used to return the heads to the inward position. The air cylinder also has a spring loaded return. This redundancy helps to ensure that in the event of failure the tool is recoverable. A coil with a board mounted Lemo was used and attached to another plate to extend the connector beyond guide rails. The final design was also cost effective to manufacture. The design for both axial and longitudinal heads is the same with exception to one machining step in the bottom of the housing. The last cut allows different magnets to be aligned and fit well. This cut can be performed last in the machining process and brings the quantity of identical heads up which pulls the individual price down. This is how the housing is easily modified to house a separate coil and magnets for either axial or circumferential direction guided waves. Urethane was used again to protect the coil from any pipe imperfections. This head design does not have a wear surface. Small bearings contact the pipe and provide a small amount of liftoff for the coil.

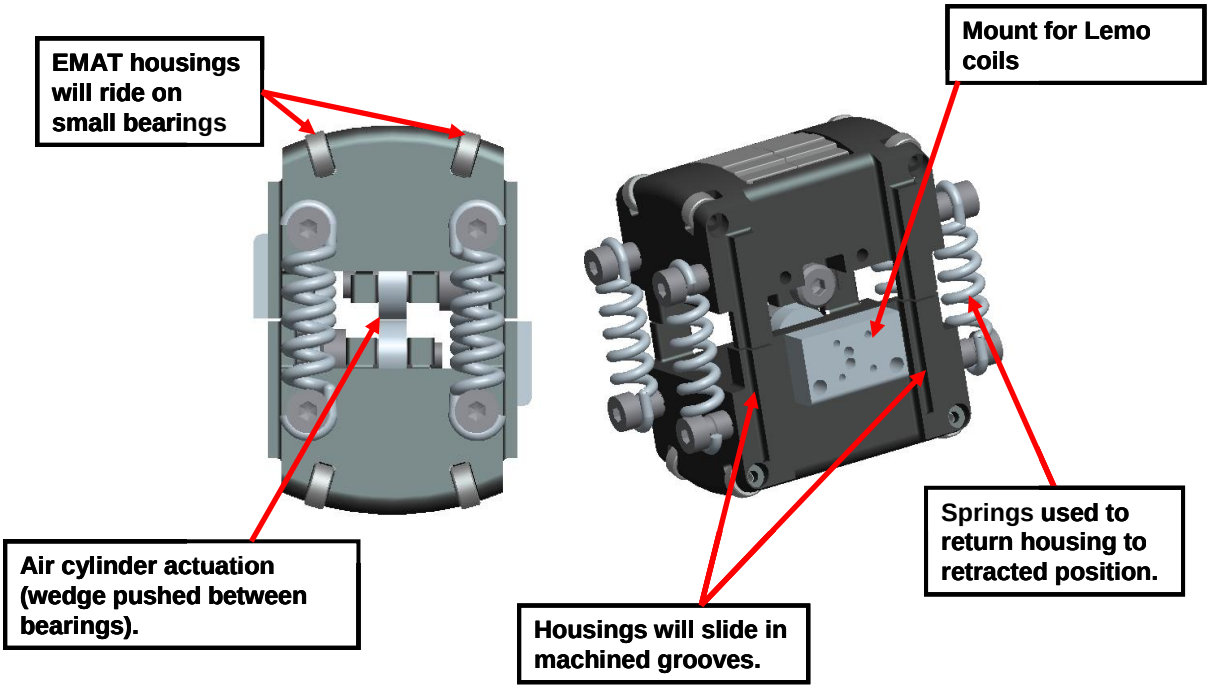

Figure 4.7 3-D component level design of the EMAT sensor heads.

One can see in Figure 4.7 that the connector mounts had to be re-engineered to accommodate clearance issues with the tool. It also is the main ground point for the wire braid to make contact directly through the pipe. This was done by changing the material to aluminum. If a positive ground is not made with the signal wire braid from all electronics directly through the pipe there will be high noise presence in the signal. The bearing ride surface will provide the ground path from the head to the pipe. Once the tool is correctly grounded to the pipe the noise level will be reduced significantly.

4.2.3 Final prototype system level design

The complete tool is comprised of two subassemblies. They are able to be used together and generate both circumferential and longitudinal direction guided waves or based on the user and detectability preference they can be separated and generate a guided wave in only one direction. Both subassemblies attached together can be seen in Figure 4.8.

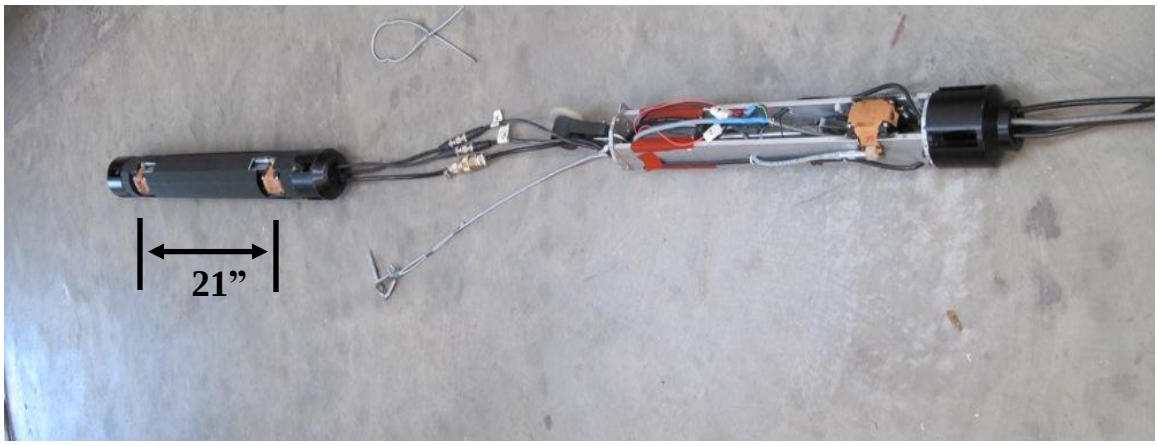

Figure 4.8 The fully assembled tool; without protective covers on the circumferential guided wave part of the tool.

Two separate pre-amps were used. One was electrically isolated to each tool. Both pre-amps were housed in the circumferential portion of the tool. Both subassemblies were pulsed simultaneously. This allowed for one external matching network to be used. The same matching network could be used for both subassemblies.

There was concern that alignment within the pipe would be a problem, so each subassembly was designed to have a suspension on both ends which can be seen on one end of the tool in Figure 4.9. There were no alignment issues so the suspension was not utilized. However, if needed the tool will have the potential to have a suspension installed on both ends of each subassembly.

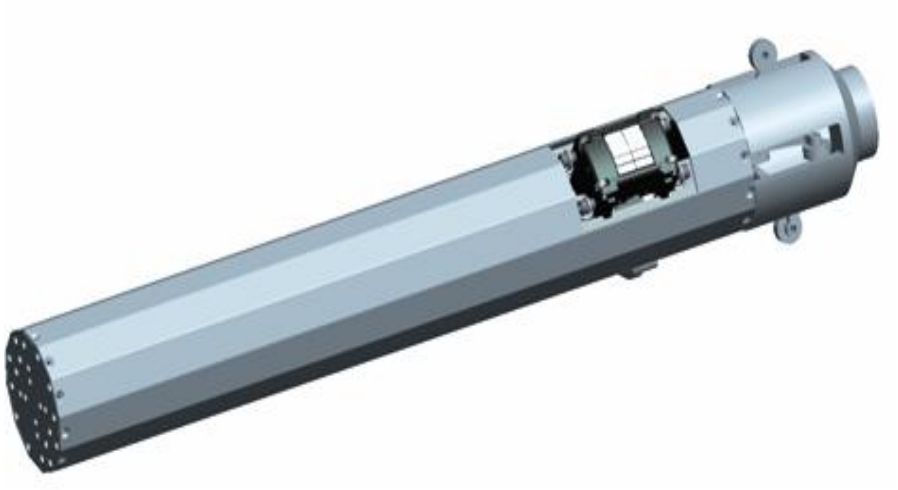

Figure 4.9 A 3-D model of the circumferential subassembly. Suspension capability in the nose cone can be seen in the upper right.

The final tool utilized air cylinders to actuate the EMAT heads outward to make contact with the pipe wall. A graphite aerosol spray was the lubricant of choice to keep the heads moving inward and outward. Each head had an orange protective urethane layer over the coil.

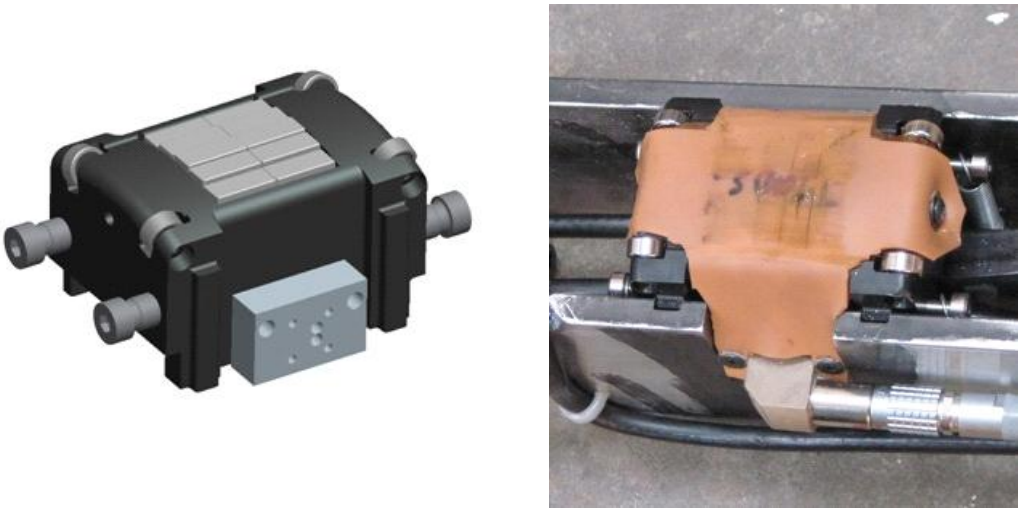

Figure 4.10 An EMAT head 3-D model is shown on the left and the final prototype is on the right.

All of the components were a very tight fit within the tool so the encoder was best mounted between both assemblies. This was anticipated since the beginning, therefore a robust encoder was chosen so this was always an option. The side by side pre-amps can be seen in Figure 4.11 along with the encoder mounted to the back of the circumferential rig.

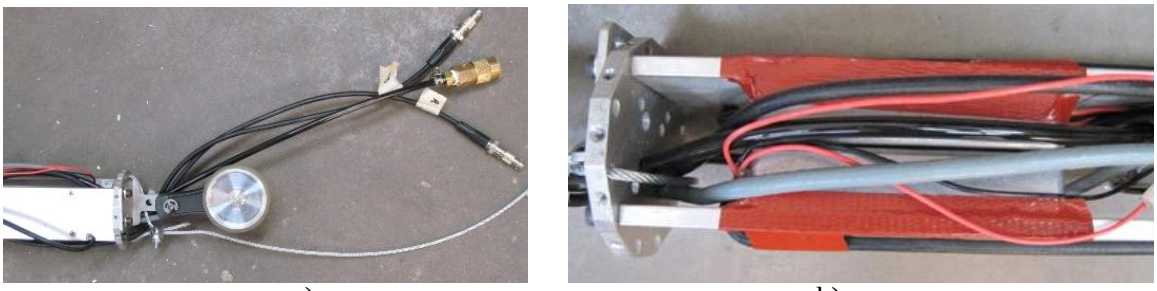

a) b)

Figure 4.11 a) The final encoder position, b) Internal pre-amps mounted internally.

The small tool had a lot packed into it; Figure 4.11 is a good representation of what little room was left over. Everything still fit in a 4-inch diameter pipe with room to allow for pipe inconsistency and obstructions. Technical drawings can be viewed in Appendix A. Bills of materials for each subassembly can be viewed in Appendix B.

4.3 Gas distribution line tool design

4.3.1 Sensor head design

The EMAT head design has been improved upon from initial designs. The magnet has a separate Noryl housing that is intended to help reduce any noise issues. Some possible noise issues from the magnet being housed in an aluminum head could be due to eddy currents being induced into the aluminum [FBS Inc., 2010]. Epoxy was used to permanently fix the magnet to the Noryl housing. The magnet housing was held in place with a separate bolt on piece that also served as the pivot and attachment point from the sensor head to the pull rig assembly. A coil "sandwich" design was used to protect the coil. This sandwich also kept the coil as close as possible to the pipe surface. A protection layer of abrasion resistant urethane was placed over the coil. The neoprene in back of the coil yields once pressure is applied to the coil. A small piece of aluminum attached the "sandwich" to the main housing through mounting holes. Leading and trailing edges of the sandwich are below the pipe contact surface. This was to prevent damage from occurring to the sensor if the sandwich would contact any pipe imperfections. Chromoly steel was used as a ride surface to contact the pipe, and to provide long tool life no other part of this head should contact the pipe.

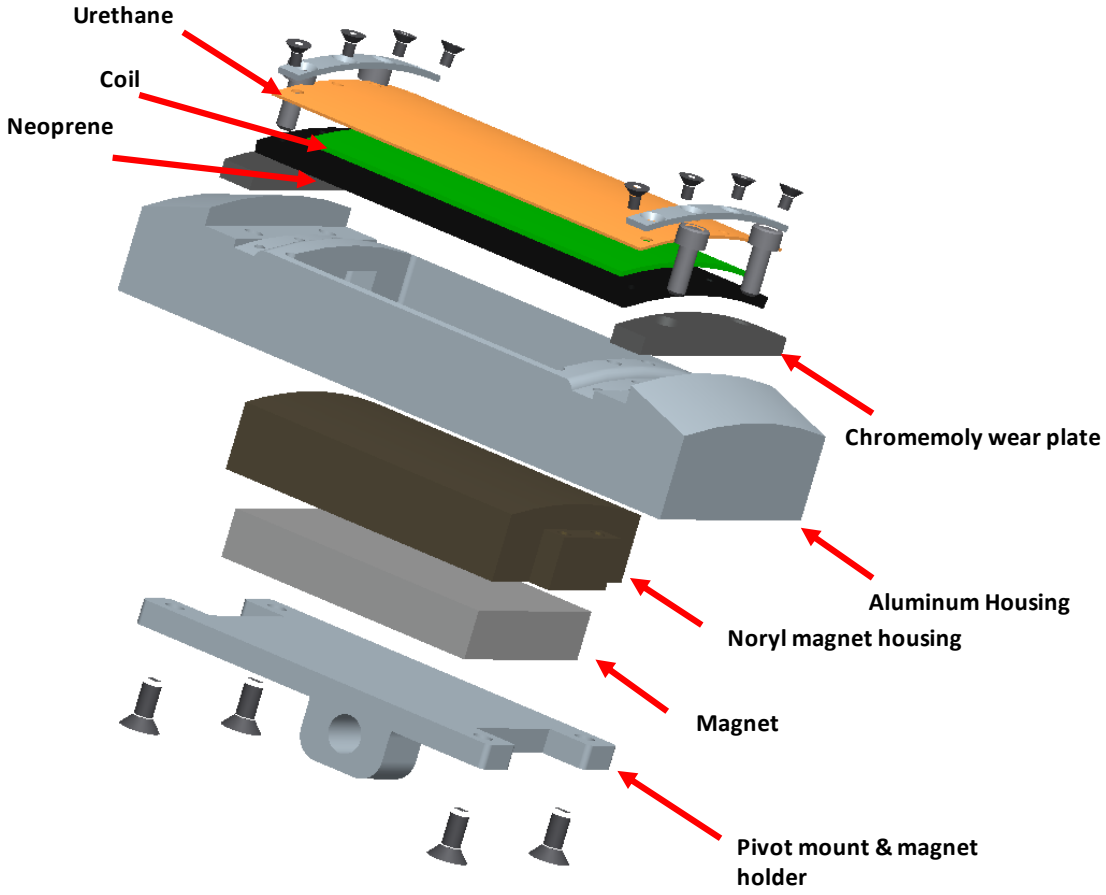

Figure 4.12 A parts diagram of an EMAT sensor head for a 12" schedule 40 pipe.

4.3.2 Cart assembly design

The pull cart was redesigned so multiple EMAT head configurations can be used. A larger head was made that houses three EMATs in one head. A "dog bone" style mount was used so that the different configurations were made more compact. Different sensor heads are put into

different positions depending on whether through transmission or pulse-echo setup was used as shown in Figures 4.13 and 4.14.

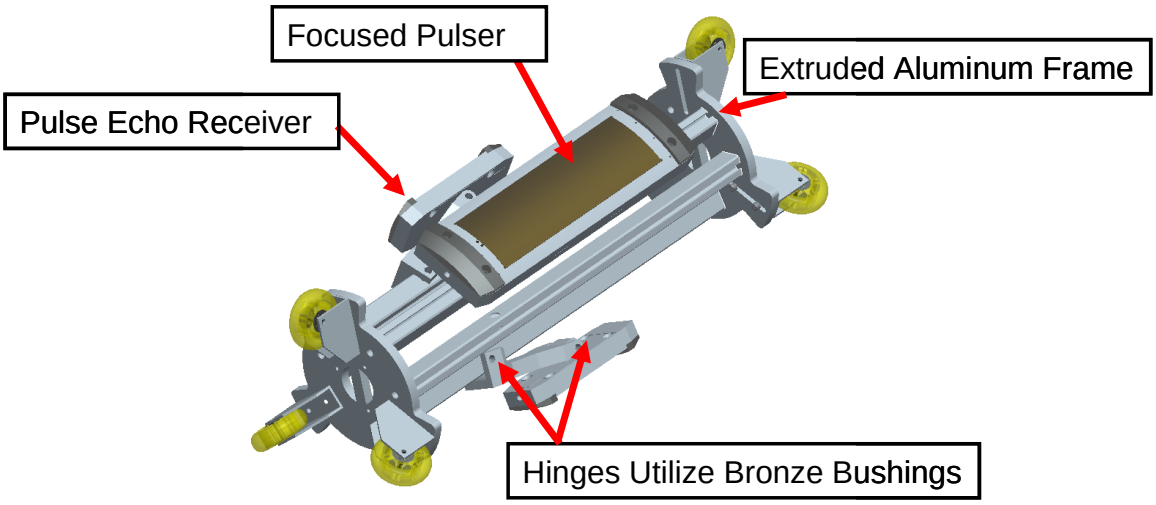

Figure 4.13 A 3-D model of the cart showing the pulse echo sensor setup.

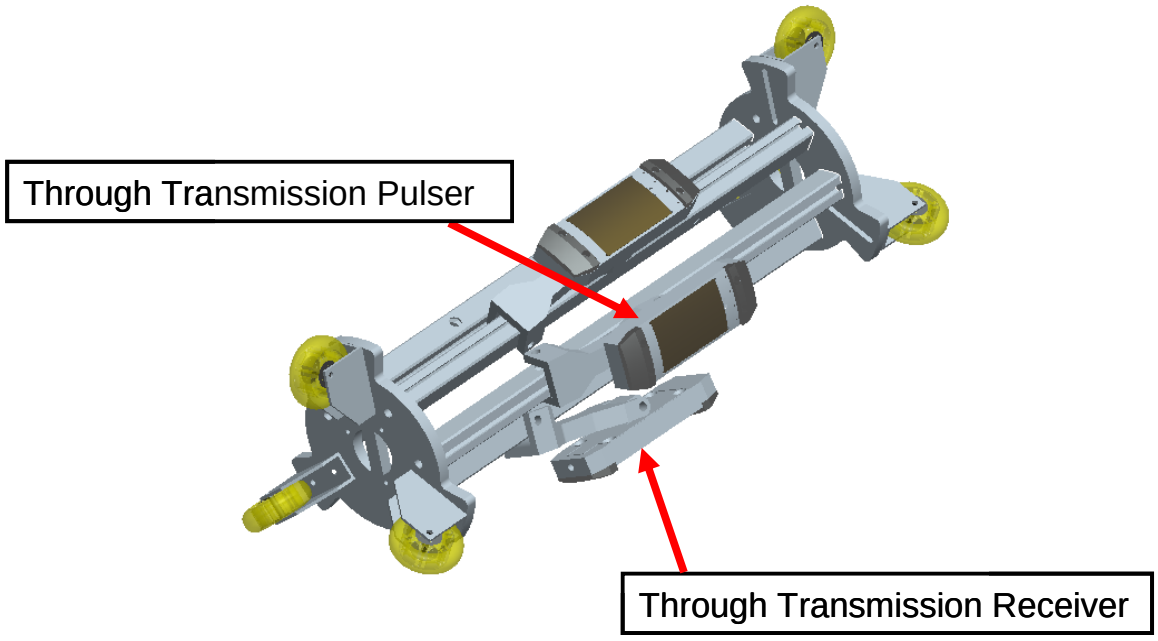

Figure 4.14 A 3-D model of the cart showing the through transmission setup.

The cart utilized prefabricated extruded aluminum to make up the frame. This off the shelf material was easy to mount and had many different configuration possibilities. The EMAT head mounts utilized bronze bushings around hinge pins to keep everything free and moving. Wheels were on separate mounts so adjustments could be made for different pipe schedules.

An encoder was again incorporated into this tool to track its position within the pipe. Two of the same preamplifier boards used in the well casing tool were used in this design. One was wired to each receiver so that data from both receiver sensors could be recorded simultaneously. Figure 4.15 shows the assembled gas distribution line tool.

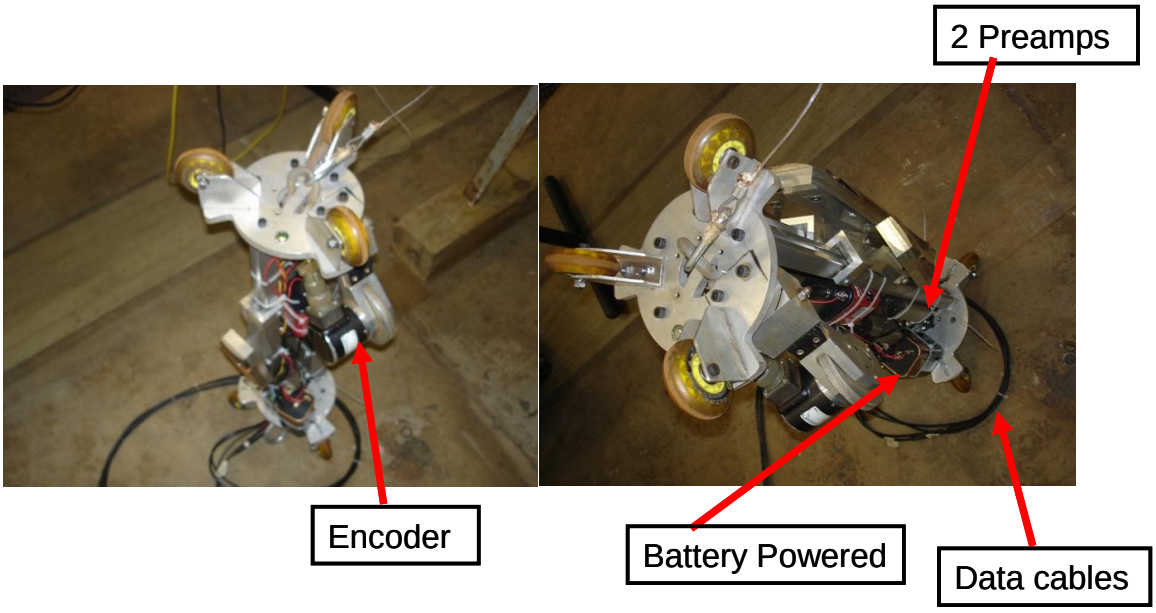

Figure 4.15 Picture of the final assembled gas distribution line tool.

Chapter 5

DEFECT CLASSIFICATION AND ANALYSIS

5.1 Goals

Once the well casing and gas distribution tools were built, the first goal was to prove the concepts and use the tools inside pipes. Any data taken would be the first time data was taken from inside a pipe farther than 12 inches. This is because these tools allow sensor placement farther inside the pipe than a human arm can reach. Different defects were studied along with their effects on the signal. The longitudinal tool was used on a saw cut defect to simulate a crack or defect in the circumferential direction. The circumferential tool was used to examine corrosion simulation defects of many sizes.

Figure 5.1 A pipe with threaded connections that experiments were performed on.

Pipes were donated to Penn State that were representative of the steel casings used in the gas storage well construction. The threaded couplings between pipe sections seen in Figure 5.1, were used in the construction of the gas storage wells.

5.2 Circumferential direction defect detection

5.2.1 Gas Storage Well

Machined defects that consisted of two drilled holes with a diameter of 0.250 inches were placed on a specimen pipe, and one example of this is shown in Figure 5.2. The circumferential sensors were tested on the defects that had a through wall depth of 30%, 50%, and 75%.

Figure 5.2 A photo showing machined defects at 50% through wall depth for a 4 inch schedule 40 pipe (0.119 inch through wall thickness defect depth).

The experiments proved to be successful in detecting the defects of the 30, 50 and 75% depths. A circumferential experiment result is shown on a clean section of pipe in Figure 5.3. Notice the multiple pipe wrap around reflections in figure 5.3.

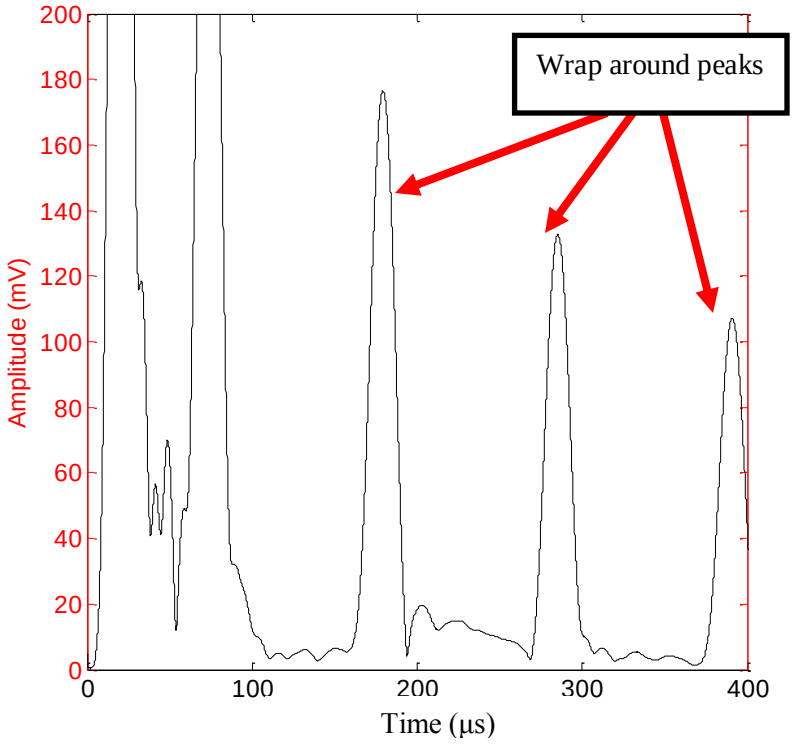

Figure 5.3 A 270 kHz circumferential signal on a clean section of 4 inch schedule 40 pipe.

The signal changes significantly with the addition of deeper defects. There is a trend of the amplitude ratio of the first wrap around signal and the highest defect peak.

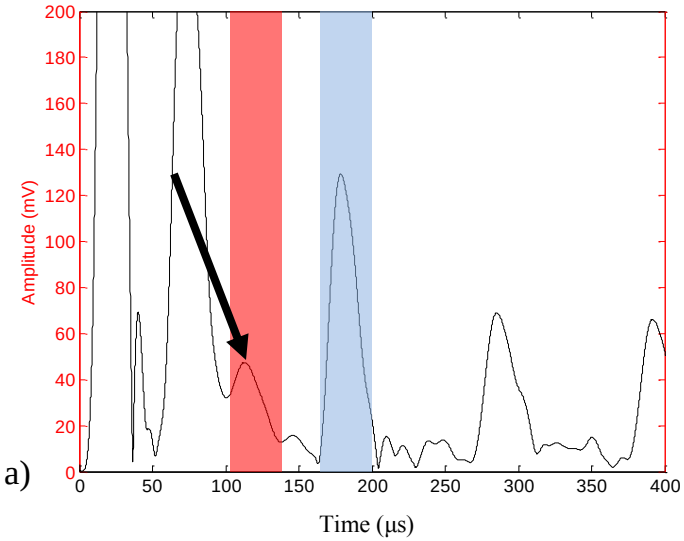

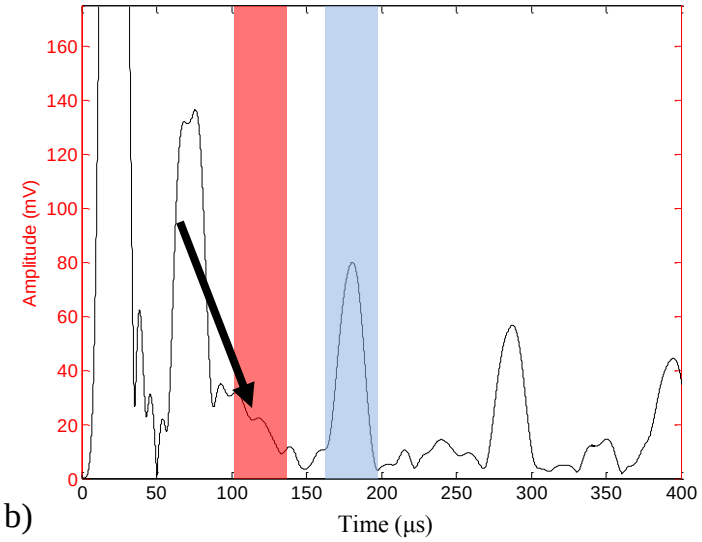

b)

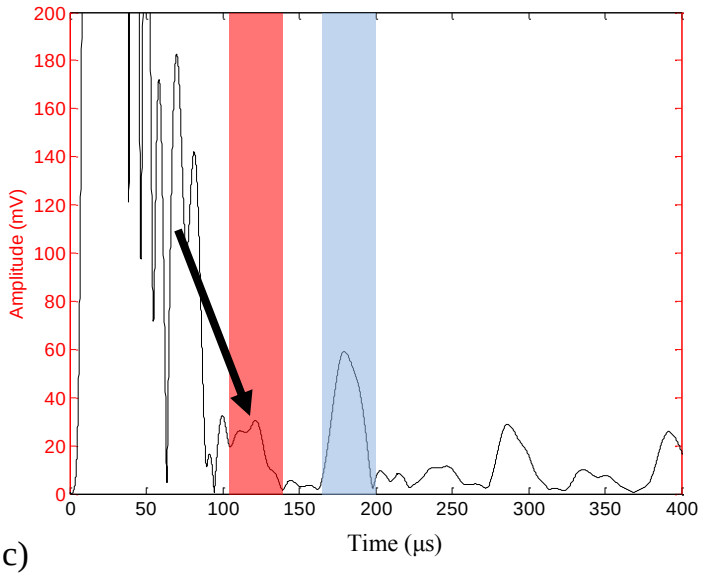

c)

Figure 5.4 Plotted signals from circumferential EMATs on various size depth defects consisting of two 0.25 inch diameter holes. a) 30% b) 50% c) 75%

Figure 5.4 shows the defect reflection highlighted in red and the first wrap around highlighted in blue. There is a correlation to defect depth with the amplitude ratio of the wrap around to the highest defect peak reflection from a time after 100-160 microseconds. Table 5.1

shows the ratios of defect reflection and wrap around reflection, the ratio corresponds with depth of defects.

Table 5.1 Peak amplitudes and an amplitude ratio shown for different depth machined defects.

scenario	wrap around peak (mv)	reflection peak (mv)	ratio
clean	176	21.8	8.07
30%	129	47	2.74
50%	80	35	2.29
75%	59	32.43	1.82

Next, a section of pipe was ground down with an electric angle grinder to simulate wall loss depth of approximately 25% through wall, as shown in Figure 5.5.

Figure 5.5 A photo of simulated wall loss caused by corrosion.

Simulated wall loss was created by grinding a 180 degree portion of the pipe. The corresponding amplitude ratio was 3.3. This ratio would fall between the 30% wall loss defect and the clean section amplitude ratio. The clean section amplitude ratio was constructed by taking the highest noise level to create the ratio.

The reason to use an amplitude ratio is that it is more reliable than defect amplitude or through transmission signal amplitude loss. A ratio is more reliable because the entire signal could have higher or lower amplitude, depending on many factors. These factors include but are not limited to sensor coupling, which has a great probability of being related to corrosion. Sensor lift off could also cause a lower signal. There could also be a higher or lower noise present in the signal because of electronic noise, or different grounding issues. Basically any time the sensor is moved many factors can result in amplitude changes.

5.2.2 Gas Distribution Line

For the through transmission setup on elongated defects a correlation is found for an amplitude ratio to defect size. The ratio of the pulse going through the defect to the pulse going in the opposite circumferential direction around the pipe for a clean section is 2.00. The ratios for the 30%, 50%, and 75% defects are 1.43, 1.04, and 0.50 respectively. When data was taken on all defects on the pipe a frequency bandwidth change it noticeable on data taken at a defect as well. This frequency bandwidth increase can help to pinpoint defect location, and the amplitude ratio can be used to determine defect severity. Figure 5.6 shows maximum amplitude and frequency bandwidth features.

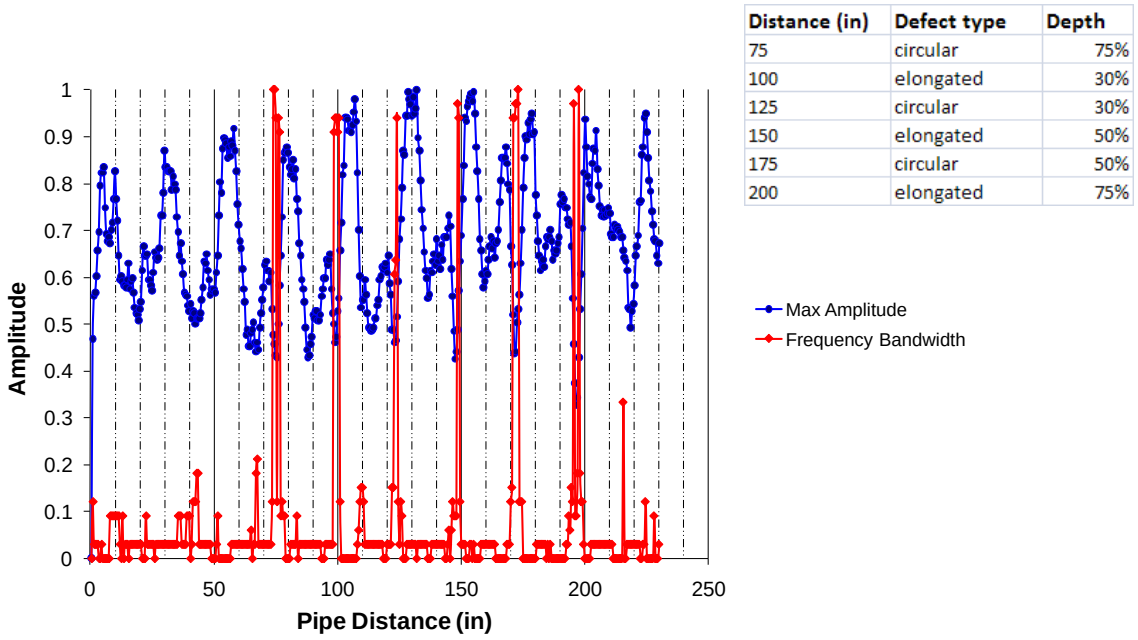

Figure 5.6 Through transmission results showing a drop in amplitude, and an increase in frequency bandwidth, at the machined defects.

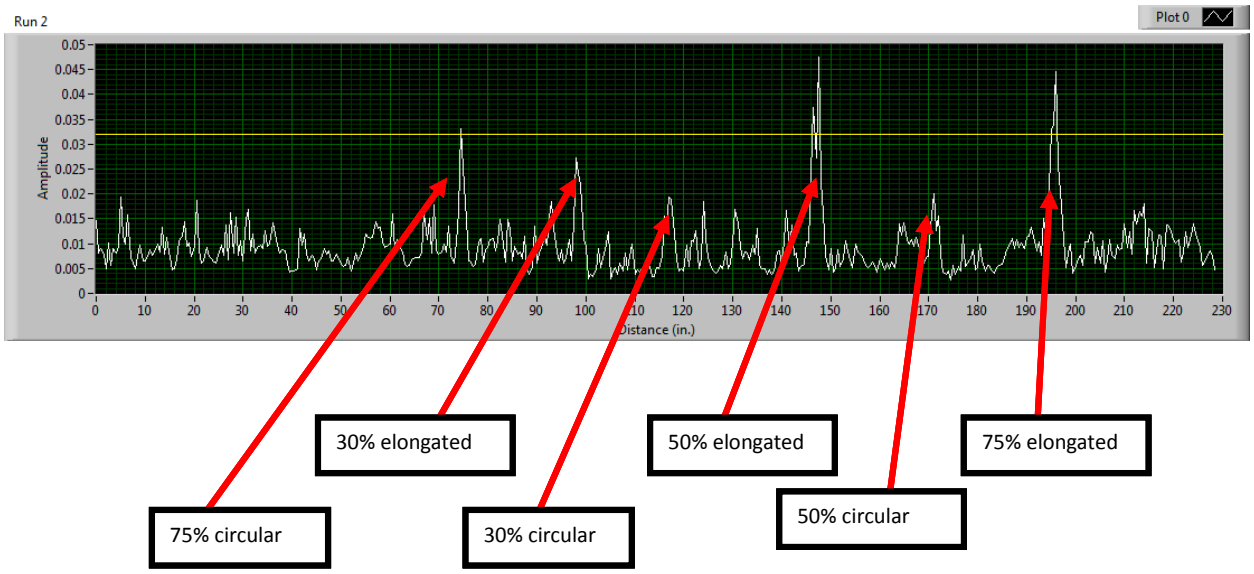

Figure 5.7 Labview processed results on a lab pipe with circular and elongated defects. [FBS Inc]

In figure 5.7 the results are defect reflections with no filtering or averaging on a 20 foot pipe. If a running average were used and filtered results before plotted against the pipe length the noise floor should be lower. When data was taken on a 20 foot section of pipe; reflections from all defects are seen. All reflections are above the noise floor. This could be one way to call out an anomaly. The circular defects are harder to detect and barely come out of the noise floor.

In the pulse echo setup if one analyzes the defect reflections you can see a different pulse shape is consistent with the type of defect as seen in Figure 5.8.

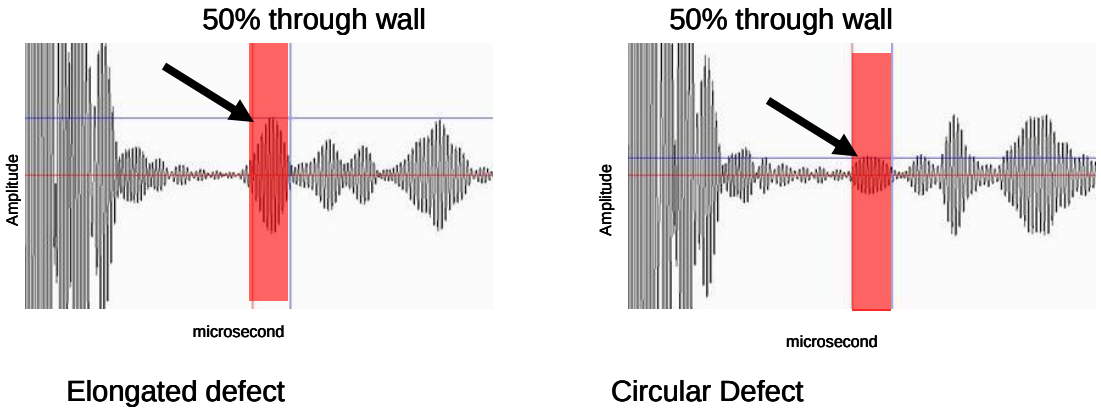

Figure 5.8 Pulse-echo results on 50% through wall conical and notch defects.

The circular defect has a smaller reflection but has a different pulse shape than the elongated defect shape. This suggests the difference in pulse shape is related to the defect shape.

Chapter 6

FIELD TESTS

6.1 Abandoned Gas Storage Well

The final totally assembled prototype was used in a field test on a decommissioned gas storage well in North Canton, Ohio.

Figure 6.1 Decommissioned gas storage well, where field tests were performed with the tool being inserted for the first time.

During the final field tests the tool proved to be very robust and reliable. Conditions were very unfavorable and the tool came out with worn wear covers and coils. Large scale and

moisture deposits were present on the tool once removed. The tool performed well throughout the testing, and yielding data for analysis. Fear of the well becoming an antenna and having a high noise content proved not to be a problem. Previous grounding issues caused high precautions to be taken with having all grounds connected to the casing, tool, and electronics. The tool was able to acquire data 100ft down into the well. This distance was only limited by the length of the coax cable used.

The first step was to insert the tool only a few feet down the well and to test all equipment to make sure everything was working as expected before a lowering the tool the full 100ft down the well. Next, at the 100ft depth the equipment was again tested. 100 foot depth signals are shown in Figures 6.2 and 6.3

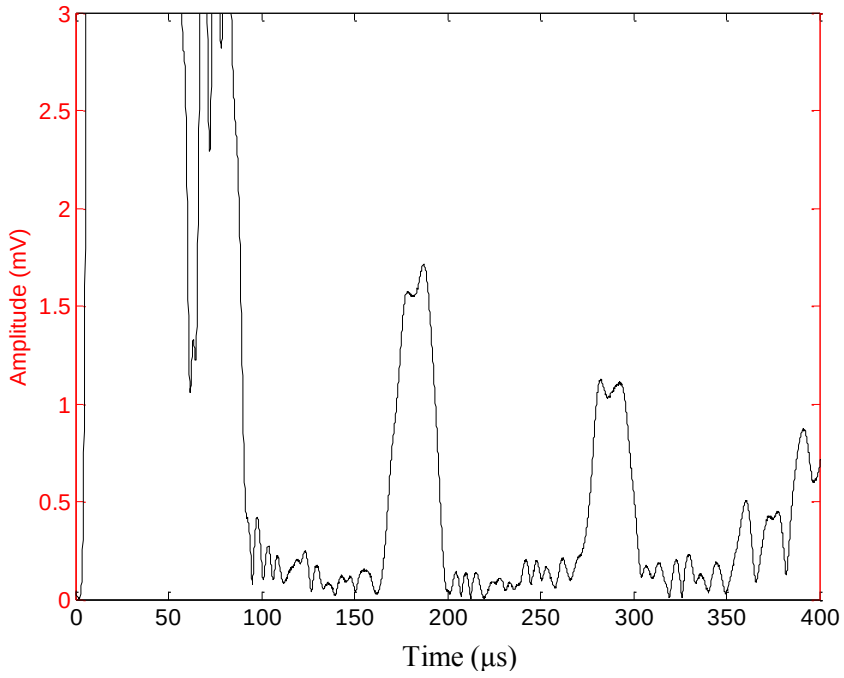

Figure 6.2 Circumferential direction sensor signal at 100ft.

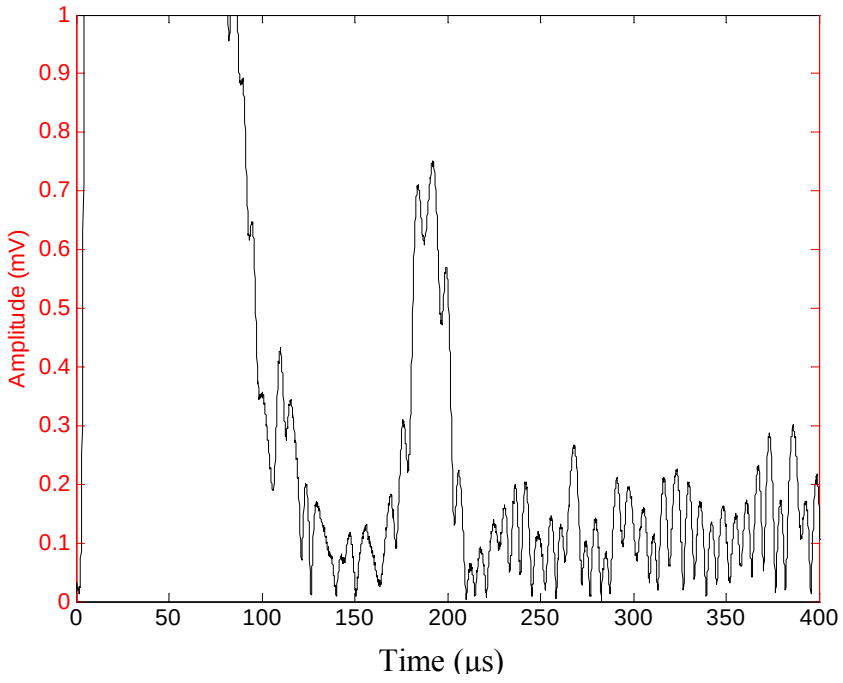

Figure 6.3 Longitudinal direction sensor signal at 100ft.

After confirming all equipment was working properly, the tool was raised up the well. Data was taken up the well casing and the signals were clear. The signals were able to be read and processed, although some rogue signals were present. It is believed that the rogue signals were present due to a bad ground to the pipe at that particular instant.

6.2 Out of Service Pipeline

After the distribution line tool was tested and successful on machined defects in the lab it was used on an out-of-service pipe with real pitting corrosion. Through transmission worked well and shows a drop in amplitude while passing though pitted sections compared to passing through clean sections as shown in Figure 6.4.

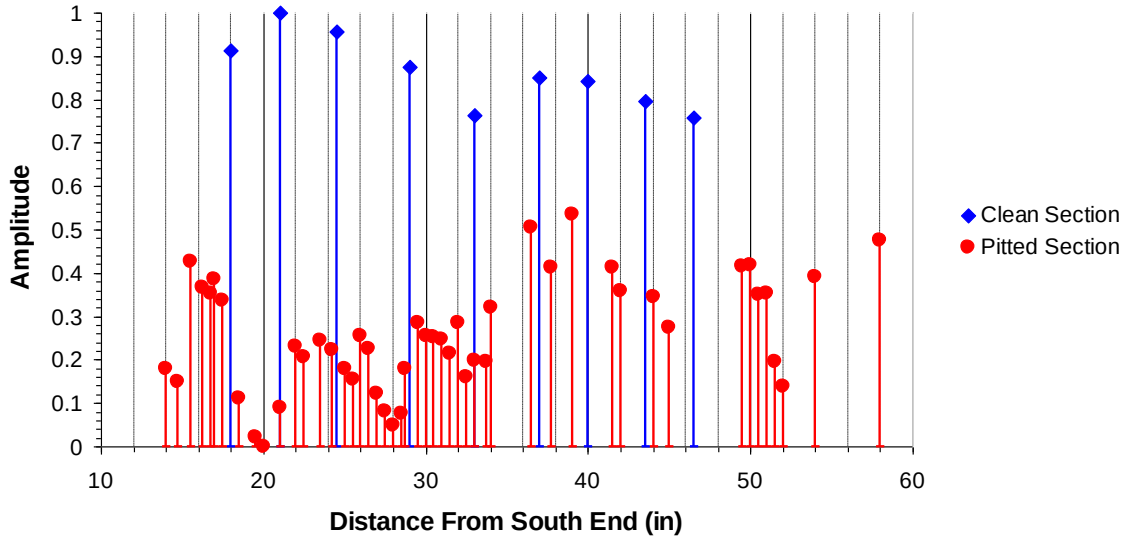

Figure 6.4 Through transmission results showing amplitude loss on defects.

The pulse-echo setup shows reflections from the defects though out the pipe as well, as presented in Figure 6.5.

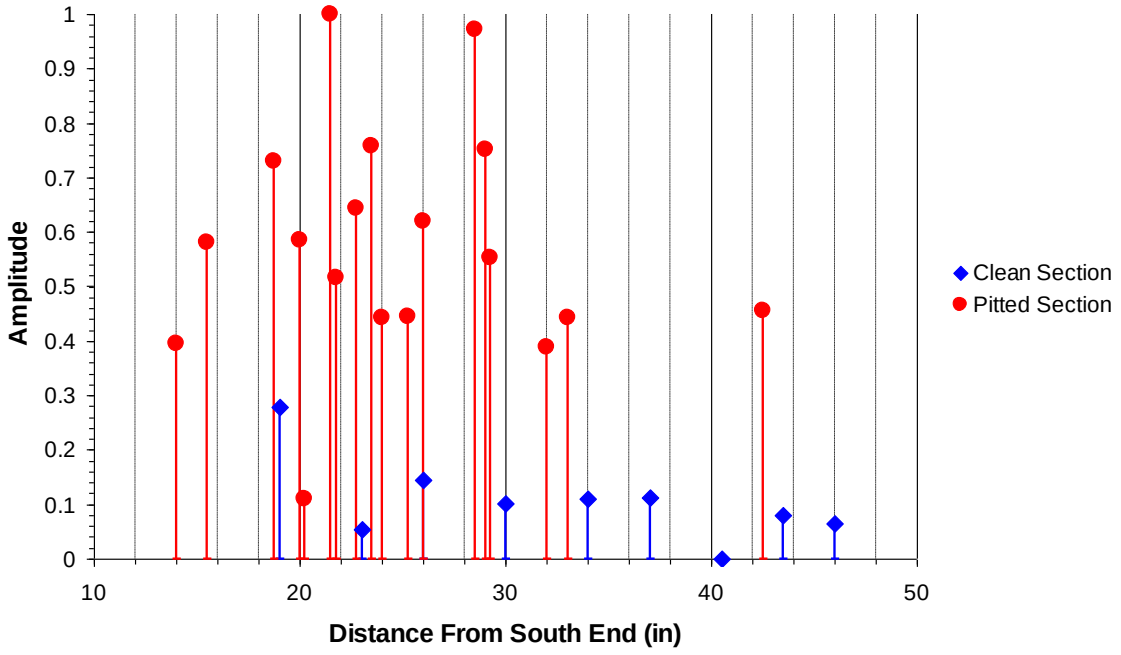

Figure 6.5 Pulse-echo results showing amplitude reflection spikes from defects; compared to the noise level of a clean section shown in blue.

Chapter 7

SUMMARY, CONCLUSIONS, AND FUTURE WORK

7.1 Gas storage well

The gas storage well tool used both circumferential and longitudinal direction guided waves. The Sensor design was chosen based on experimental results. The guided waves were implemented from the inside of the steel well casing with a prototype tool. The tool utilized the final sensor designs. Using the tool, position of the sensors can be tracked and defects detected. Successful results were obtained on lab pipes to determine the final tool capability, as well as a successful field test with data collection and tool operation inside of a decommissioned well.

Defect detection and depth of the defect can be estimated with the tool. Field tests were performed and the tool held up well during data collection was performed.

There are improvements to be made in the next phases of the technology development. After using the prototype there are some design improvement possibilities. It should be made easier to take apart and clean. The tool should be made more environmentally sealed. Protective urethane cover sizes should be adjusted to account for wear. One air cylinder failed, the cause was unknown and not attributed to the tool design. To prevent any misalignment of the EMAT heads grooves were used. Smooth operation of the heads is critical. This could be done more efficiently with the heads mounted on sliders with a PTFE material sleeve. Careful material choices and design improvements would also prevent frequent cleanings between uses.

Grounding brushes being added to the tool could help insure a better ground at all times. After the field test, it was determined that the well casing should be cleaned before the tool is used. This will dislodge any loose corrosion that would damage the sensors. The pre-amps could

be better packaged and more connectors added. This will insure there will not be any wiring issues.

In the future, a software program made specifically to control the tool would be advantageous. One feature would be to detect bad signals and record another waveform at that instant. This would enable data for that portion of the casing to be available no matter what the circumstance.

The addition of wireless data transmission is needed. To go much further than 100 feet this is needed due to low voltage signals. With any long length of wire, a low voltage signal can be quickly eliminated. Other problems may arise once wireless capabilities are added, such as the casing acting as an antenna and adding more noise to the signal.

7.2 Pitting corrosion tool

The corrosion of highest interest is circular pitting. Circular pitting appears in lines axially along a pipeline. Current methods of detecting this type of corrosion are insufficient. An EMAT sensor design was chosen and the frequency and mode of highest defect detection sensitivity were chosen experimentally through a theoretical driven background. A prototype tool was build and used inside 12" pipes with machined and natural corrosion. The machined corrosion pipe was used in lab experiments; a natural corrosion specimen was a pipe that was taken out of service due to it's poor condition.

The experiments were a success. The EMATS can detect all desired defects. In through transmission, frequency bandwidth increases on all defects consistently. The amplitude ratio of a pulse through the defect compared to not through the defect correlates with defect size. An EMAT will lend it self nicely to tool automation later due to the no couplant requirement. This knowledge could be used later in the development of a tool that would screen critical pipes and produce accurate results of pitting corrosion presence. Being able to do this could save lives, prevent environmental hazards, and save money.

A look into defect reflection shapes should be taken. This information could help in the classification of defect shape. A more robust software should be used that would filter and average waveforms before plotting along pipe length.

Appendix A

TECHNICAL DRAWINGS

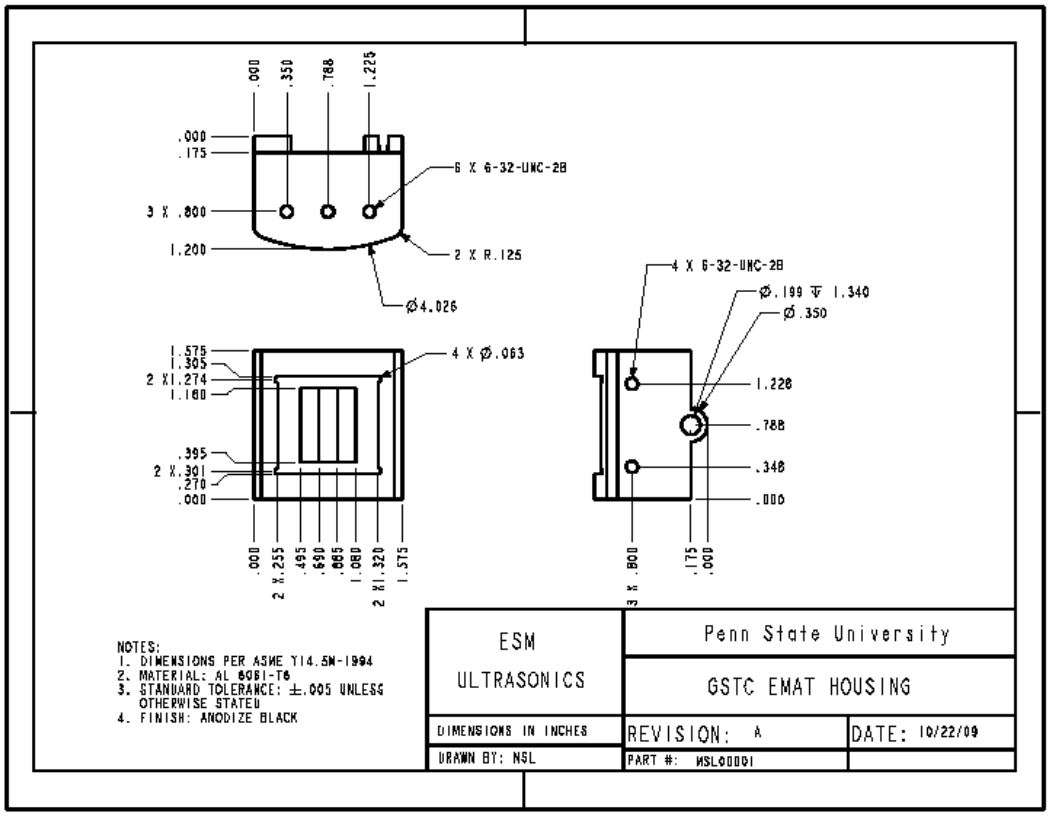

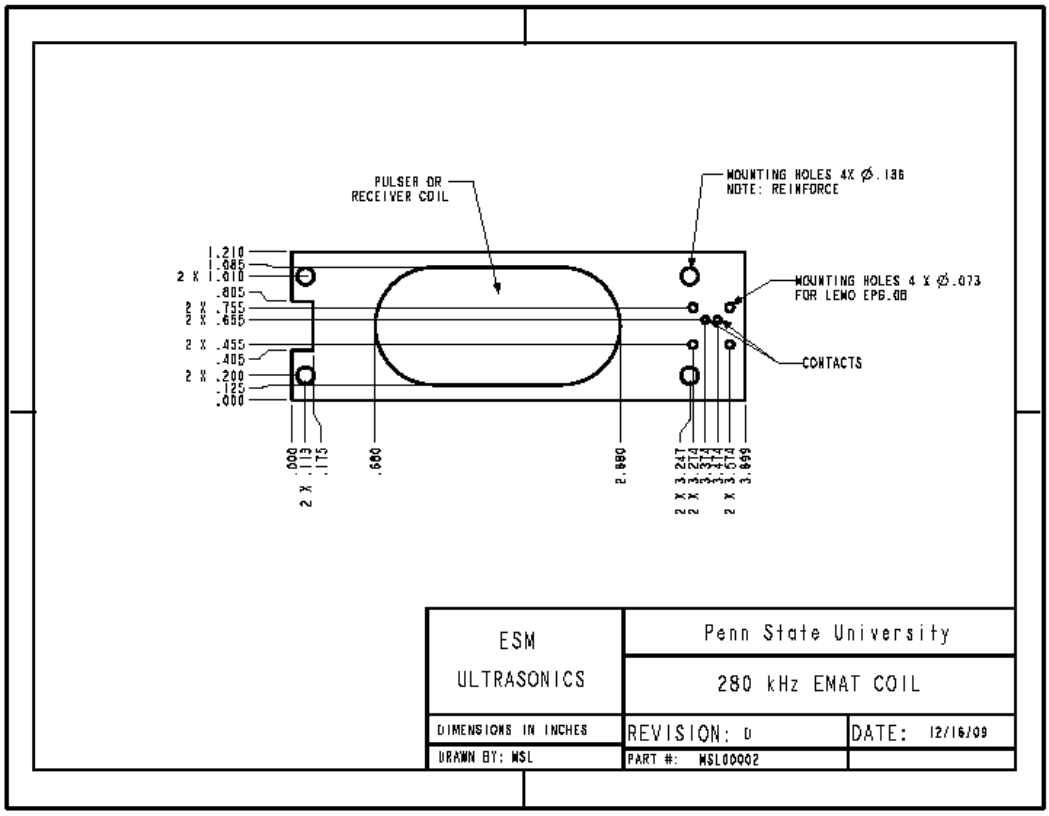
PULSER OR
RECEIVER COIL
MOUNTING HOLES 4X Ø.136
NOTE: REINFORCE
MOUNTING HOLES 4 X Ø.073
FOR LEMO EP6.0B
CONTACTS
1.210
1.085
2 X 1.010
.805
2 X .755
2 X .655
2 X .455
.405
2 X .200
.125
.000
.000
2 X .113
.175
.680
2.880
2 X 3.247
2 X 3.374
3.474
3.574
2 X 3.674
3.899
ESM
ULTRASONICS
Penn State University
280 kHz EMAT COIL
DIMENSIONS IN INCHES
REVISION: D
DATE: 12/16/09
DRAWN BY: MSL
PART #: MSL00002

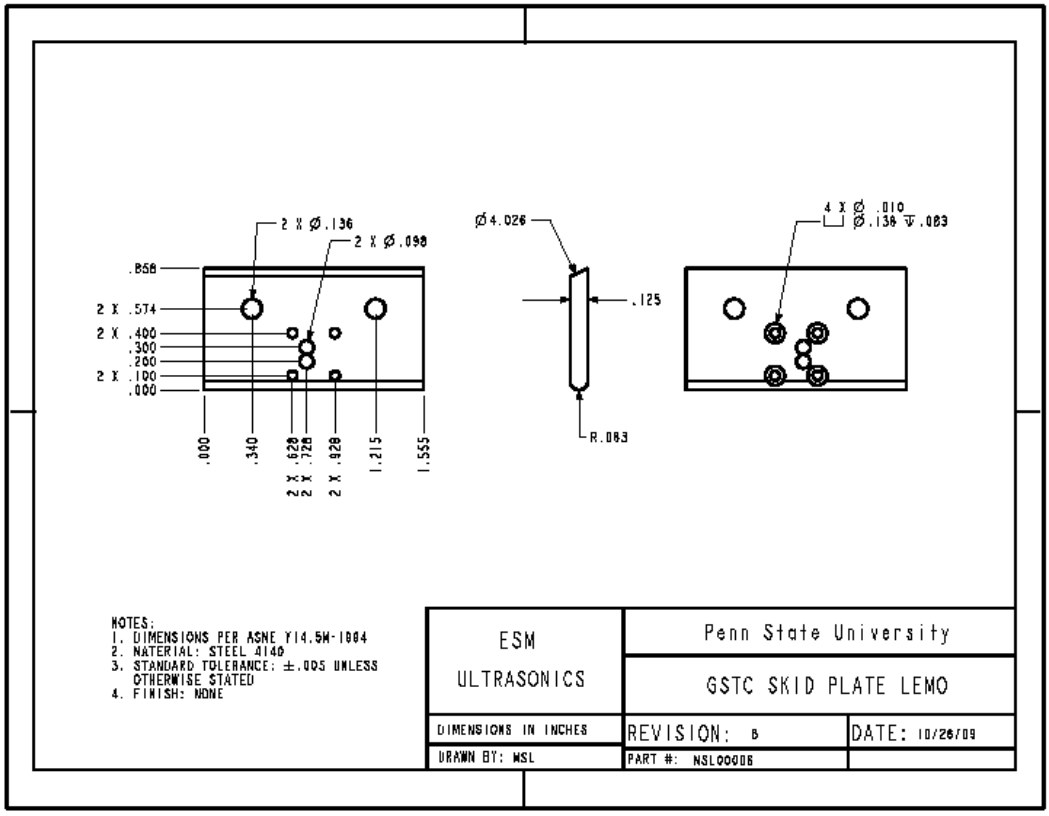
2 X Ø.136
2 X Ø.098
.858
2 X .574
2 X .400
.300
.200
2 X .100
.000
.000
.340
2 X .628
2 X .728
2 X .928
1.215
1.555
Ø4.026
.125
R.083
4 X Ø .010
Ø.138 ↧ .083
NOTES:
1. DIMENSIONS PER ASME Y14.5M-1994
2. MATERIAL: STEEL 4140
3. STANDARD TOLERANCE: ±.005 UNLESS OTHERWISE STATED
4. FINISH: NONE
ESM
ULTRASONICS
Penn State University
GSTC SKID PLATE LEMO
DIMENSIONS IN INCHES
REVISION: B
DATE: 10/26/09
DRAWN BY: MSL
PART #: NSL000006

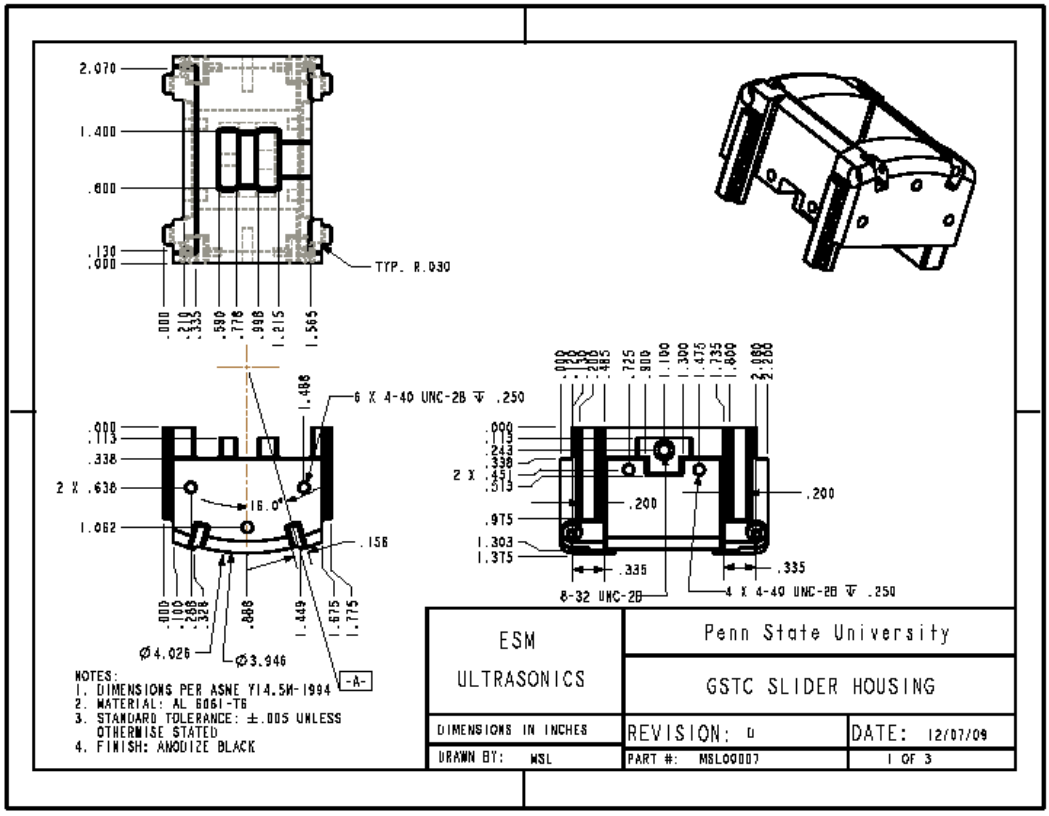
2.070
1.400
.600
.130
.000
TYP. R.030
.000
.210
.335
.590
.778
.998
1.215
1.565
1.488
6 X 4-40 UNC-2B ↧ .250
.000
.113
.338
2 X .638
16.0°
1.062
.156
.000
.100
.208
.328
.888
1.449
1.675
1.775
Ø4.026
Ø3.946
-A-
.000
.113
.243
.338
2 X .451
.513
.975
1.303
1.375
.725
.900
1.100
1.300
1.475
1.735
1.800
2.088
2.288
.200
.200
.335
.335
8-32 UNC-2B
4 X 4-40 UNC-2B ↧ .250
NOTES:
1. DIMENSIONS PER ASME Y14.5M-1994
2. MATERIAL: AL 6061-T6
3. STANDARD TOLERANCE: ±.005 UNLESS OTHERWISE STATED
4. FINISH: ANODIZE BLACK
ESM
ULTRASONICS
Penn State University
GSTC SLIDER HOUSING
DIMENSIONS IN INCHES
REVISION: D
DATE: 12/07/09
DRAWN BY: WSL
PART #: MSL0D007
1 OF 3

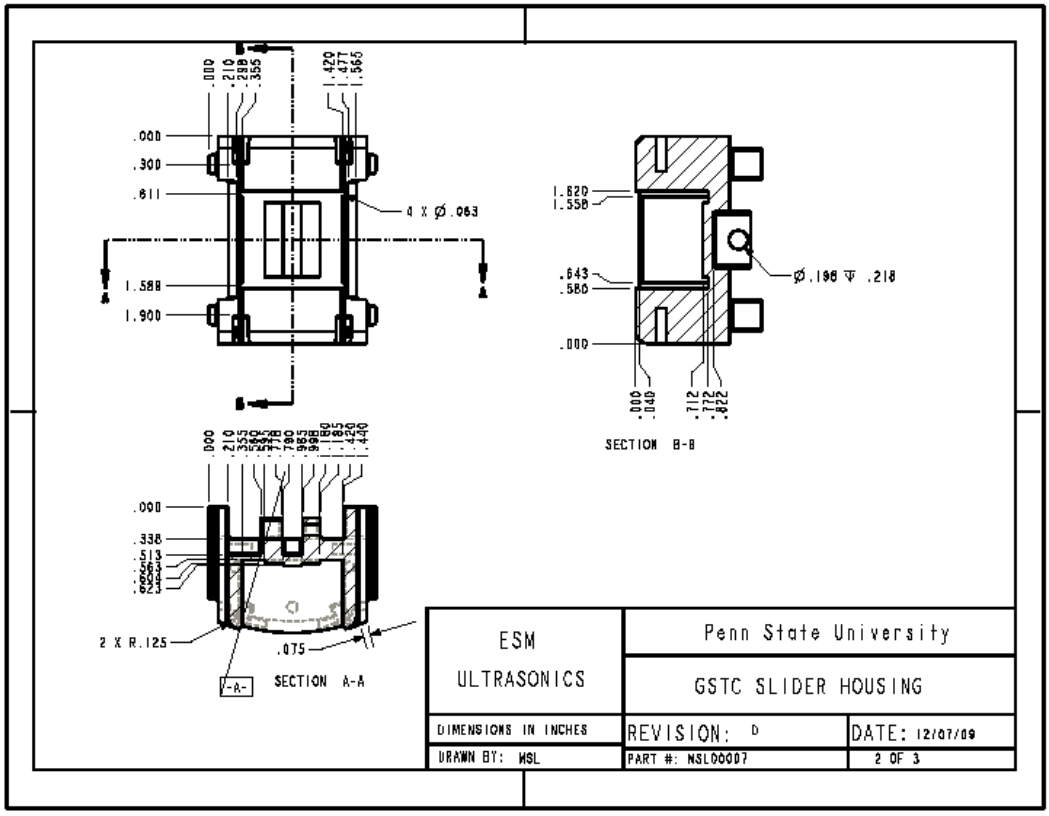
.000
.210
.298
.355
1.420
1.477
1.565
.000
.300
.611
4 X Ø.063
1.588
1.900
1.820
1.558
.643
.580
.000
Ø.196 ⌅ .218
.000
.048
.712
.772
.822
SECTION B-B
.000
.210
.355
.513
.000
.338
.513
2 X R.125
.075
V-A-
SECTION A-A
ESM
ULTRASONICS
Penn State University
GSTC SLIDER HOUSING
DIMENSIONS IN INCHES
REVISION: D
DATE: 12/07/09
DRAWN BY: MSL
PART #: NSL00007
2 OF 3

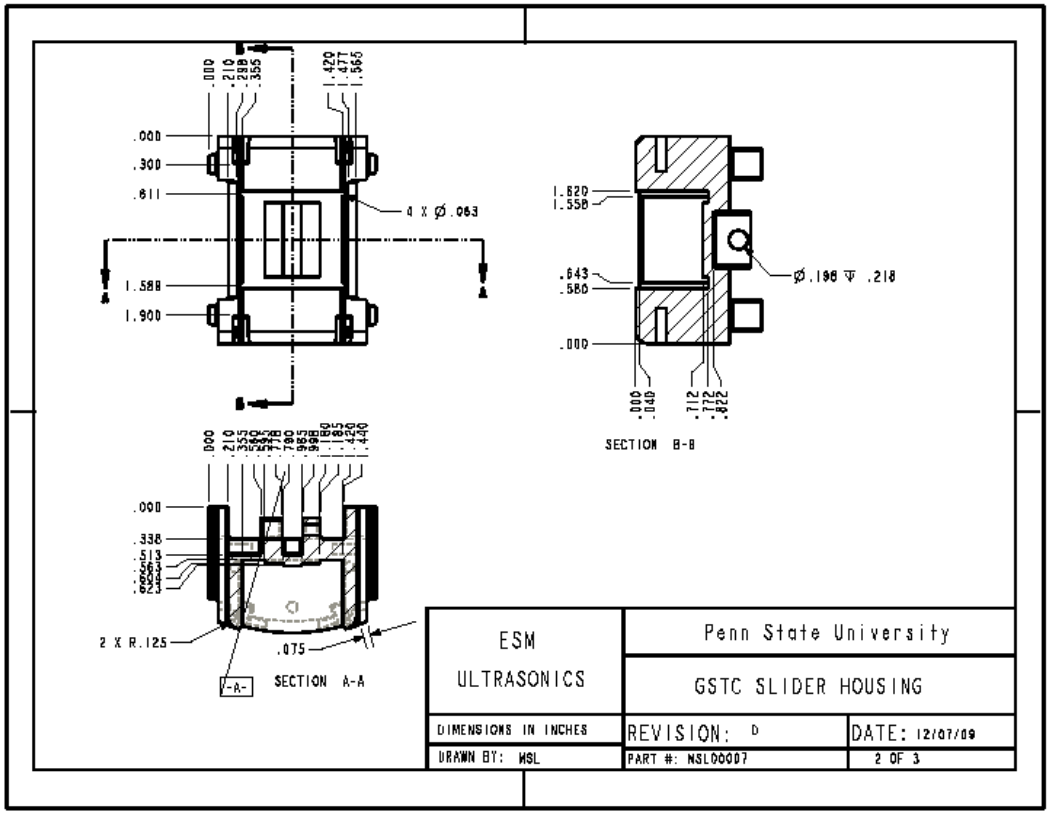
4 X Ø.063
SECTION B-B
Ø.196 ↧ .218
2 X R.125
.075
SECTION A-A
ESM
ULTRASONICS
Penn State University
GSTC SLIDER HOUSING
DIMENSIONS IN INCHES
REVISION: D
DATE: 12/07/09
DRAWN BY: MSL
PART #: NSL00007
2 OF 3

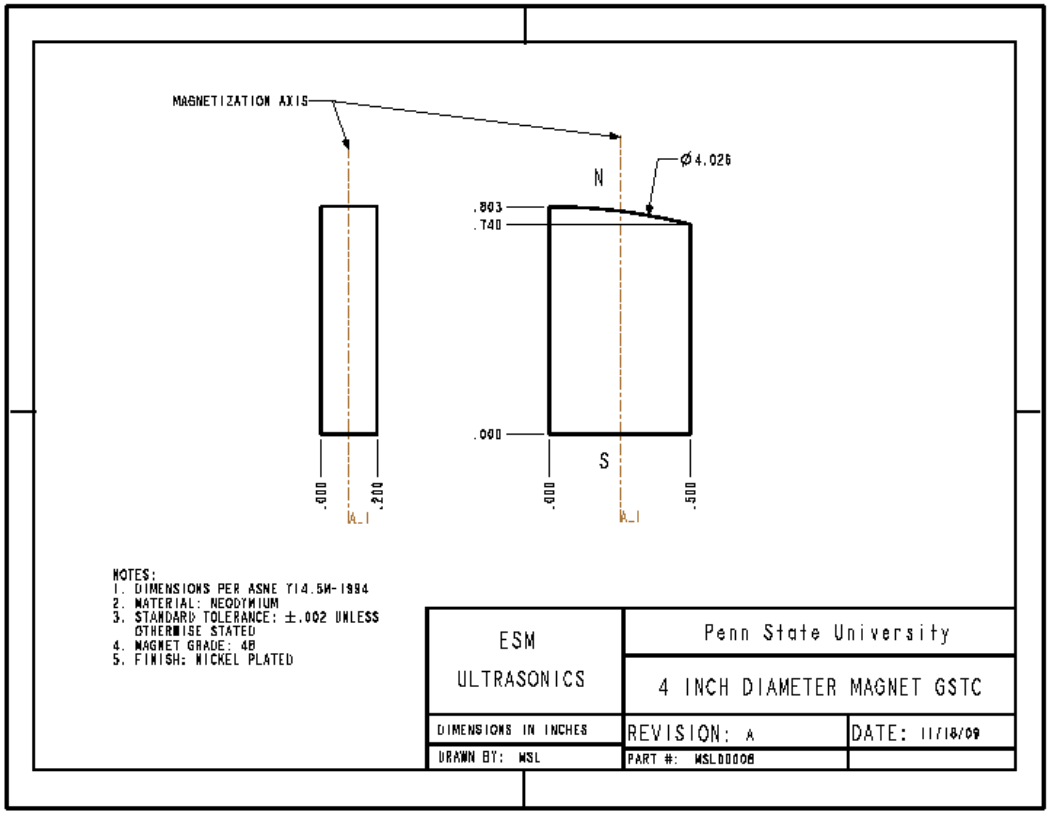
MAGNETIZATION AXIS
Ø4.026
N
.803
.740
.000
S
.000
.200
.000
.500
NOTES:
1. DIMENSIONS PER ASME Y14.5M-1994
2. MATERIAL: NEODYMIUM
3. STANDARD TOLERANCE: ±.002 UNLESS OTHERWISE STATED
4. MAGNET GRADE: 48
5. FINISH: NICKEL PLATED
ESM ULTRASONICS
Penn State University
4 INCH DIAMETER MAGNET GSTC
DIMENSIONS IN INCHES
REVISION: A
DATE: 11/18/09
DRAWN BY: WSL
PART #: WSL00008

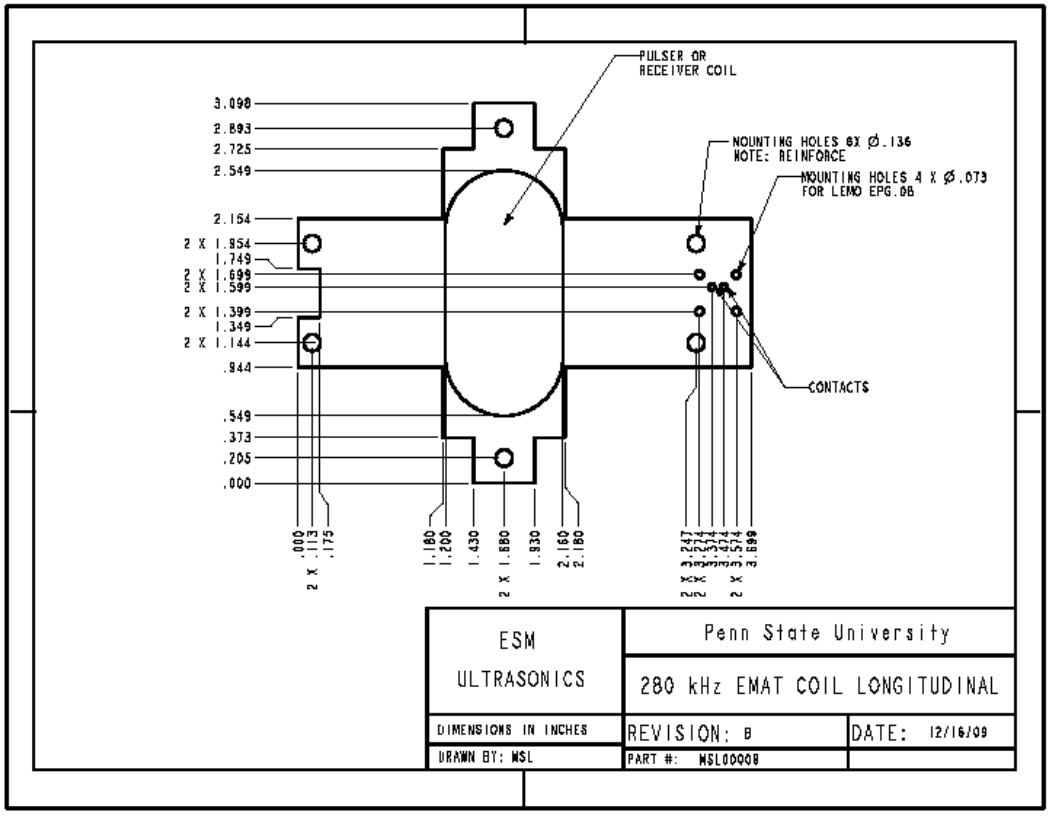
PULSER OR
RECEIVER COIL
MOUNTING HOLES 6X Ø.136
NOTE: REINFORCE
MOUNTING HOLES 4 X Ø.073
FOR LEMO EPG.0B
CONTACTS
3.098
2.893
2.725
2.549
2.154
2 X 1.954
1.749
2 X 1.699
2 X 1.599
2 X 1.399
1.349
2 X 1.144
.944
.549
.373
.205
.000
2 X .000
.113
.175
1.180
1.200
1.430
2 X 1.880
1.930
2.160
2.180
2 X 3.247
3.274
3.374
3.474
3.574
2 X 3.699
ESM
ULTRASONICS
Penn State University
280 kHz EMAT COIL LONGITUDINAL
DIMENSIONS IN INCHES
REVISION: B
DATE: 12/16/09
DRAWN BY: MSL
PART #: MSL00008

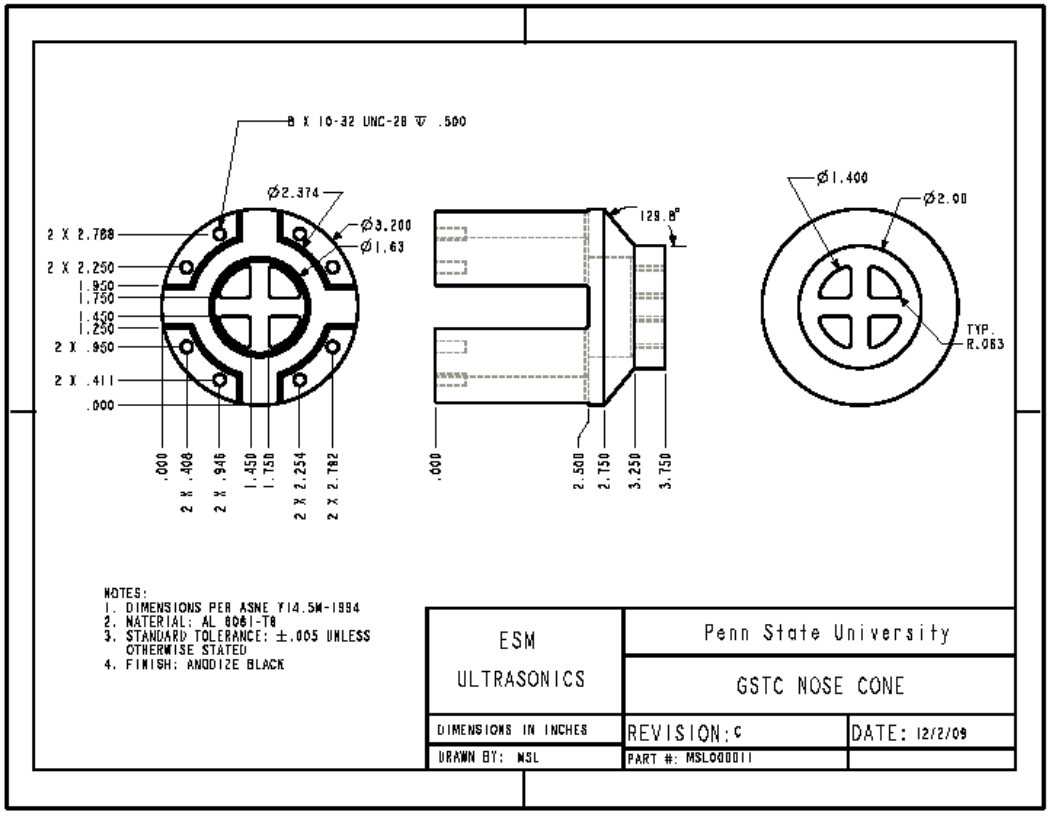
8 X 10-32 UNC-2B ↧ .500
Ø2.374
Ø3.200
Ø1.63
2 X 2.788
2 X 2.250
1.950
1.750
1.450
1.250
2 X .950
2 X .411
.000
.000
2 X .408
2 X .946
1.450
1.750
2 X 2.254
2 X 2.782
129.8°
.000
2.500
2.750
3.250
3.750
Ø1.400
Ø2.00
TYP.
R.063
NOTES:
1. DIMENSIONS PER ASME Y14.5M-1994
2. MATERIAL: AL 6061-T6
3. STANDARD TOLERANCE: ±.005 UNLESS OTHERWISE STATED
4. FINISH: ANODIZE BLACK
ESM
ULTRASONICS
Penn State University
GSTC NOSE CONE
DIMENSIONS IN INCHES
REVISION: C
DATE: 12/2/09
DRAWN BY: MSL
PART #: MSL0600011

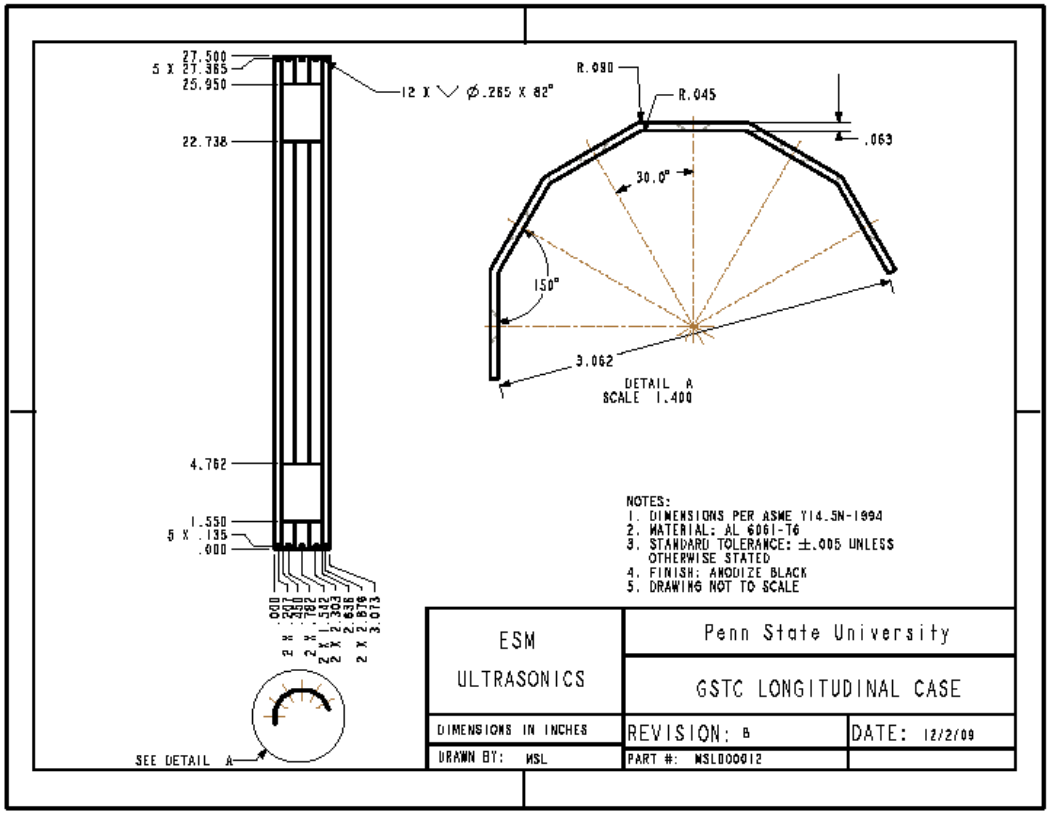
27.500
5 X 27.385
25.950
12 X ∨ Ø.285 X 82°
22.738
4.762
1.550
5 X .135
.000
.000
.217
.410
2 X .782
2 X 1.542
2 X 2.303
2 X 2.636
2 X 2.879
3.073
SEE DETAIL A
R.080
R.045
.063
30.0°
150°
3.062
DETAIL A
SCALE 1.400
NOTES:
1. DIMENSIONS PER ASME Y14.5M-1994
2. MATERIAL: AL 6061-T6
3. STANDARD TOLERANCE: ±.005 UNLESS OTHERWISE STATED
4. FINISH: ANODIZE BLACK
5. DRAWING NOT TO SCALE
ESM ULTRASONICS
Penn State University
GSTC LONGITUDINAL CASE
DIMENSIONS IN INCHES
REVISION: B
DATE: 12/2/09
DRAWN BY: MSL
PART #: MSL000012

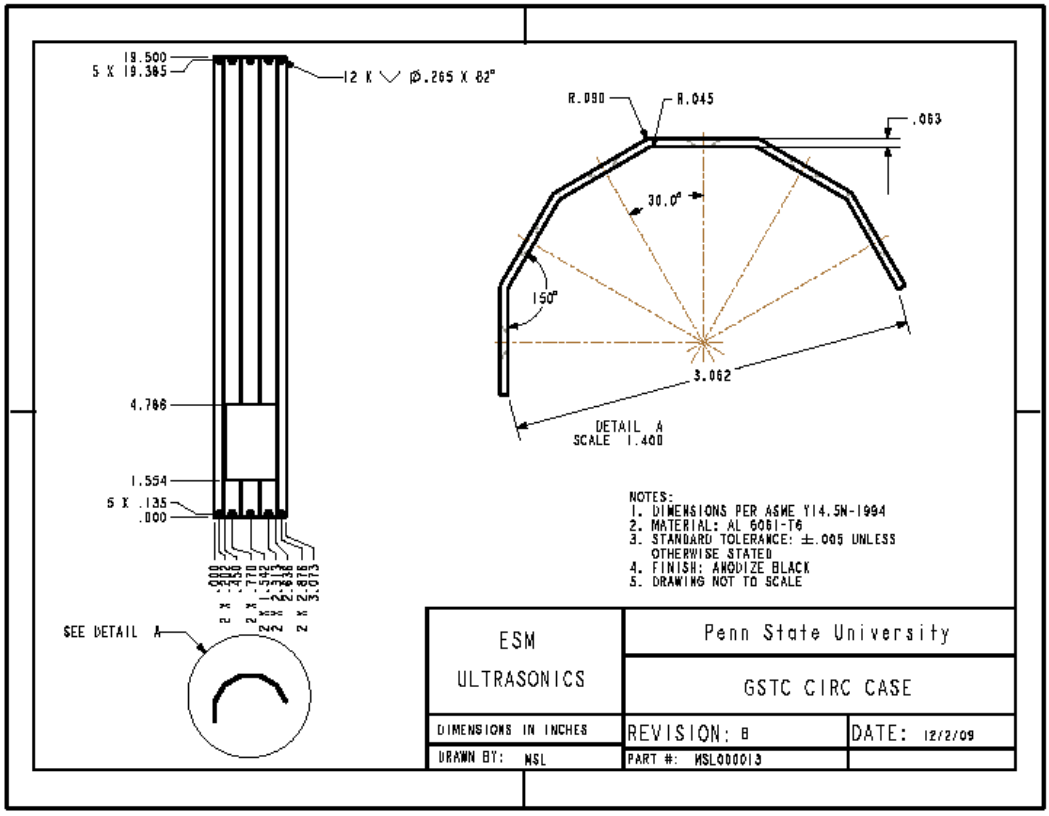
18.500
5 X 19.385
12 X ⌵ Ø.265 X 82°
R.090
R.045
.063
30.0°
150°
3.062
DETAIL A
SCALE 1.400
4.788
1.554
5 X .135
.000
SEE DETAIL A
NOTES:
1. DIMENSIONS PER ASME Y14.5M-1994
2. MATERIAL: AL 6061-T6
3. STANDARD TOLERANCE: ±.005 UNLESS OTHERWISE STATED
4. FINISH: ANODIZE BLACK
5. DRAWING NOT TO SCALE
ESM ULTRASONICS
Penn State University
GSTC CIRC CASE
DIMENSIONS IN INCHES
REVISION: B
DATE: 12/2/09
DRAWN BY: MSL
PART #: MSL000013

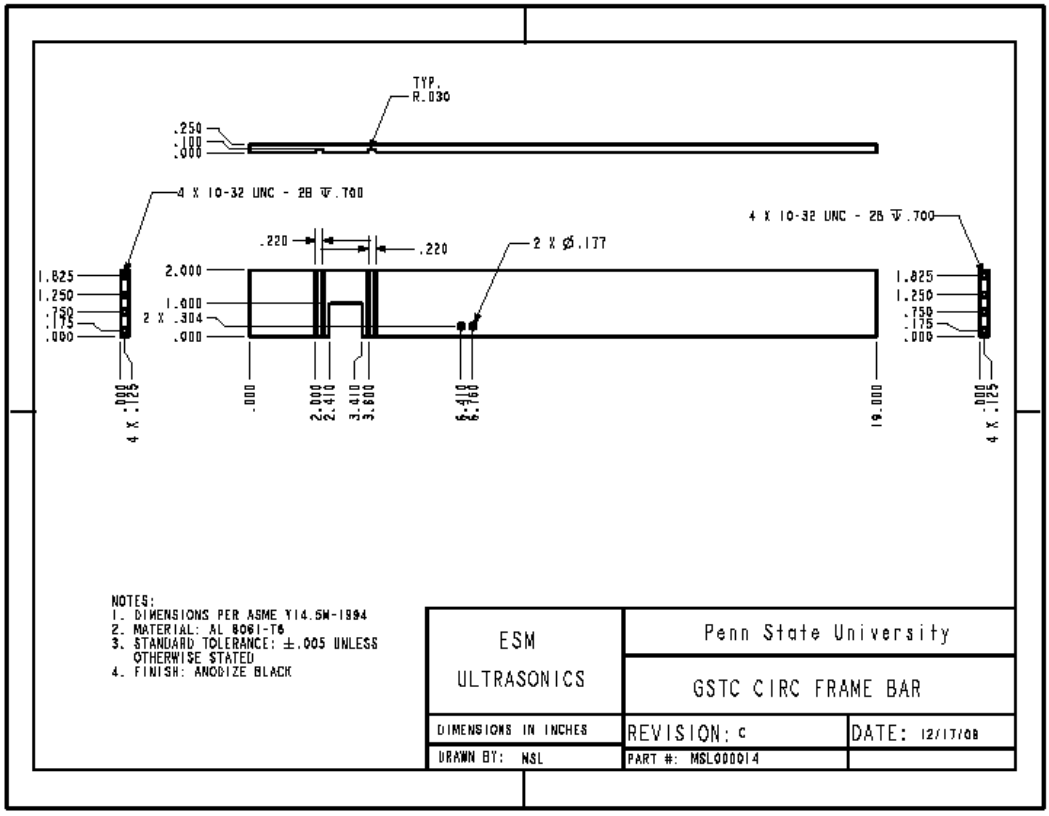

NOTES:
1. DIMENSIONS PER ASME Y14.5M-1994
2. MATERIAL: AL 6061-T6
3. STANDARD TOLERANCE: ±.005 UNLESS OTHERWISE STATED
4. FINISH: ANODIZE BLACK

ESM ULTRASONICS	Penn State University	
	GSTC CIRC FRAME BAR	
DIMENSIONS IN INCHES	REVISION: C	DATE: 12/17/08
DRAWN BY: NSL	PART #: MSL000014	

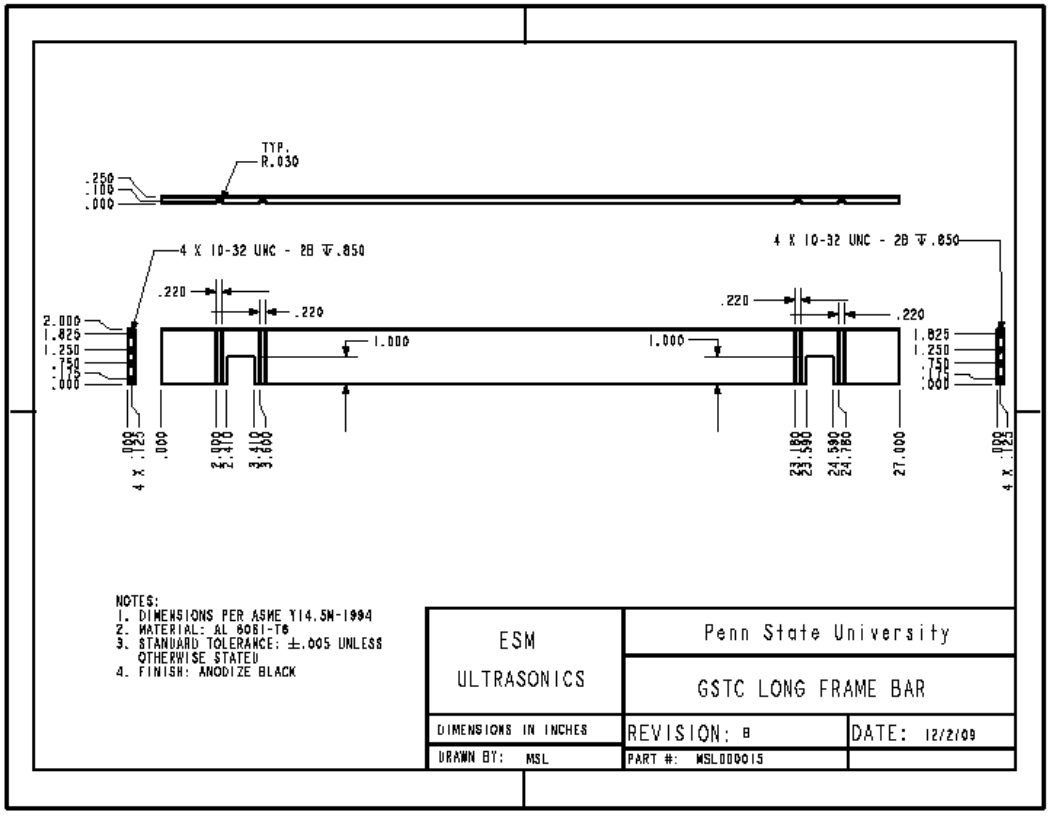
TYP.
R.030
.250
.100
.000
4 X 10-32 UNC - 2B ↧.850
4 X 10-32 UNC - 2B ↧.850
.220
.220
.220
.220
2.000
1.825
1.250
.750
.500
.000
1.000
1.000
1.825
1.250
.750
.500
.000
4 X .125 .000
2.000 2.476
3.410 3.660
23.180 23.580
24.580 24.780
27.000
4 X .125
NOTES:
1. DIMENSIONS PER ASME Y14.5M-1994
2. MATERIAL: AL 6061-T6
3. STANDARD TOLERANCE: ±.005 UNLESS OTHERWISE STATED
4. FINISH: ANODIZE BLACK
ESM
ULTRASONICS
Penn State University
GSTC LONG FRAME BAR
DIMENSIONS IN INCHES
REVISION: B
DATE: 12/2/09
DRAWN BY: MSL
PART #: MSL000015

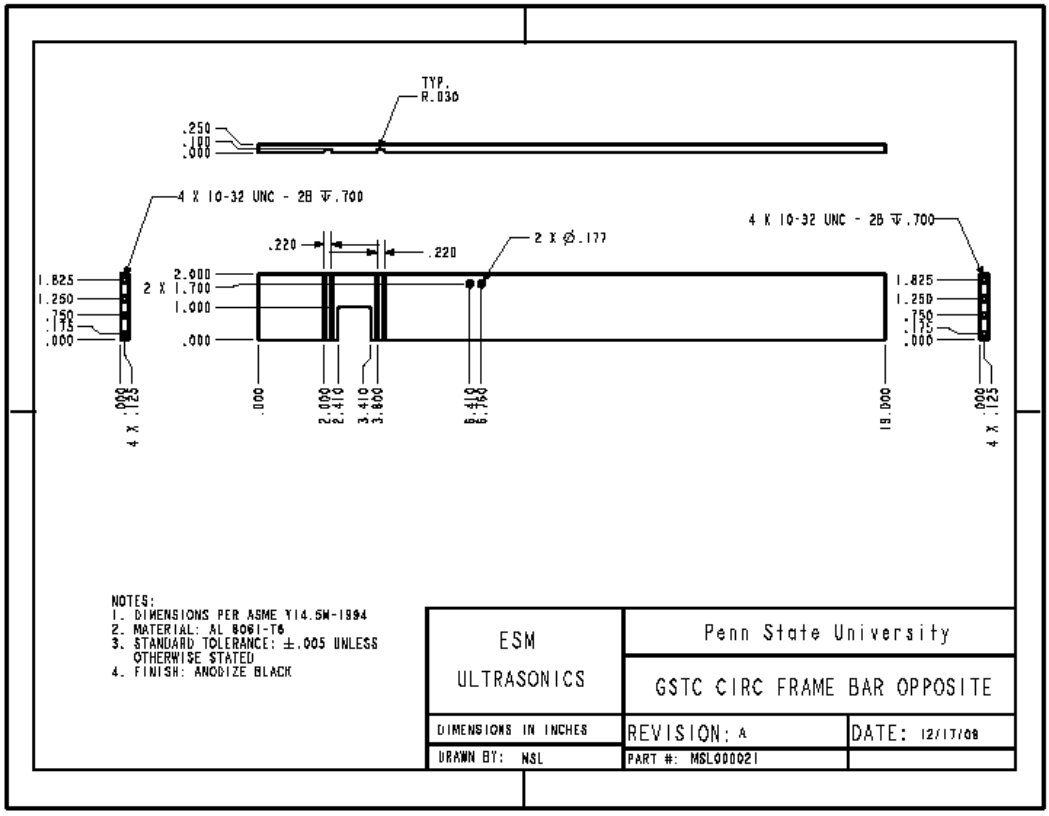
TYP.
R.030
.250
.100
.000
4 X 10-32 UNC - 2B ↧.700
4 X 10-32 UNC - 2B ↧.700
.220
.220
2 X Ø.177
1.825
1.250
.750
.175
.000
2.000
2 X 1.700
1.000
.000
19.000
4 X .125
2.000
2.410
3.410
3.800
6.410
6.790
NOTES:
1. DIMENSIONS PER ASME Y14.5M-1994
2. MATERIAL: AL 6061-T6
3. STANDARD TOLERANCE: ±.005 UNLESS OTHERWISE STATED
4. FINISH: ANODIZE BLACK
ESM
ULTRASONICS
Penn State University
GSTC CIRC FRAME BAR OPPOSITE
DIMENSIONS IN INCHES
REVISION: A
DATE: 12/17/08
DRAWN BY: NSL
PART #: MSL000021

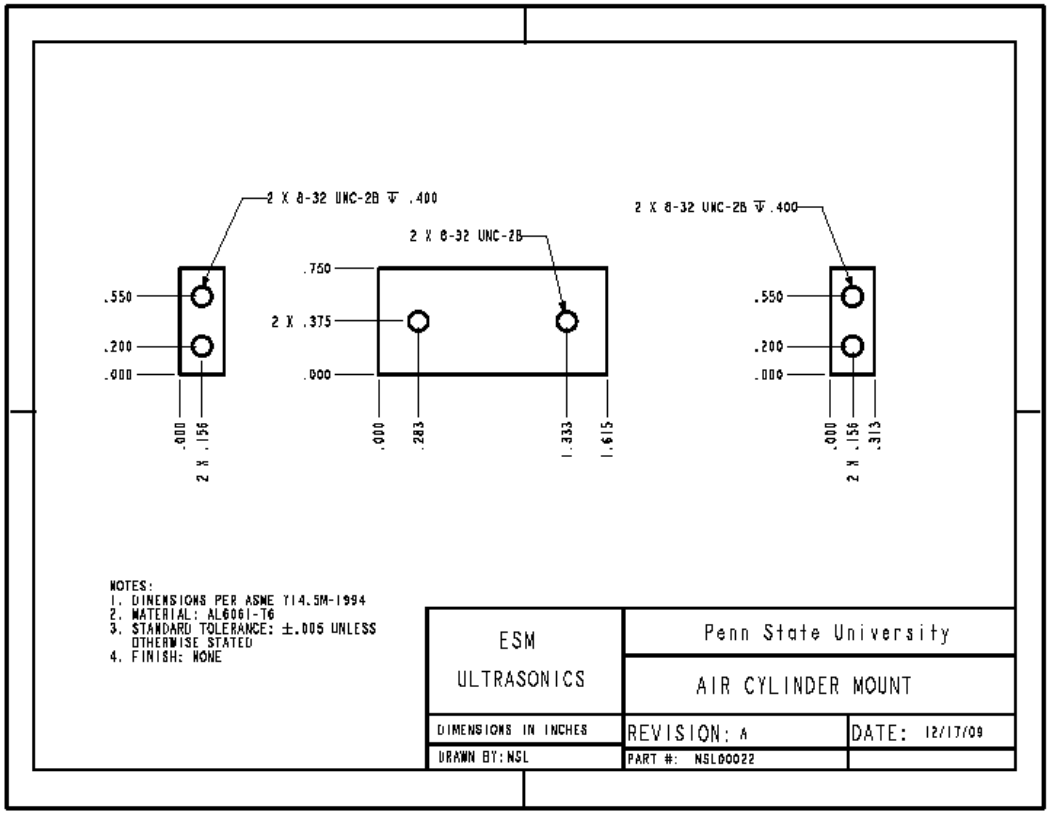
2 X 8-32 UNC-2B ↧ .400
2 X 8-32 UNC-2B
2 X 8-32 UNC-2B ↧ .400
.750
2 X .375
.000
.550
.200
.000
.000
2 X .156
.000
.283
1.333
1.615
.550
.200
.000
.000
2 X .156
.313
NOTES:
1. DIMENSIONS PER ASME Y14.5M-1994
2. MATERIAL: AL6061-T6
3. STANDARD TOLERANCE: ±.005 UNLESS OTHERWISE STATED
4. FINISH: NONE
ESM
ULTRASONICS
Penn State University
AIR CYLINDER MOUNT
DIMENSIONS IN INCHES
REVISION: A
DATE: 12/17/09
DRAWN BY: NSL
PART #: NSL00022

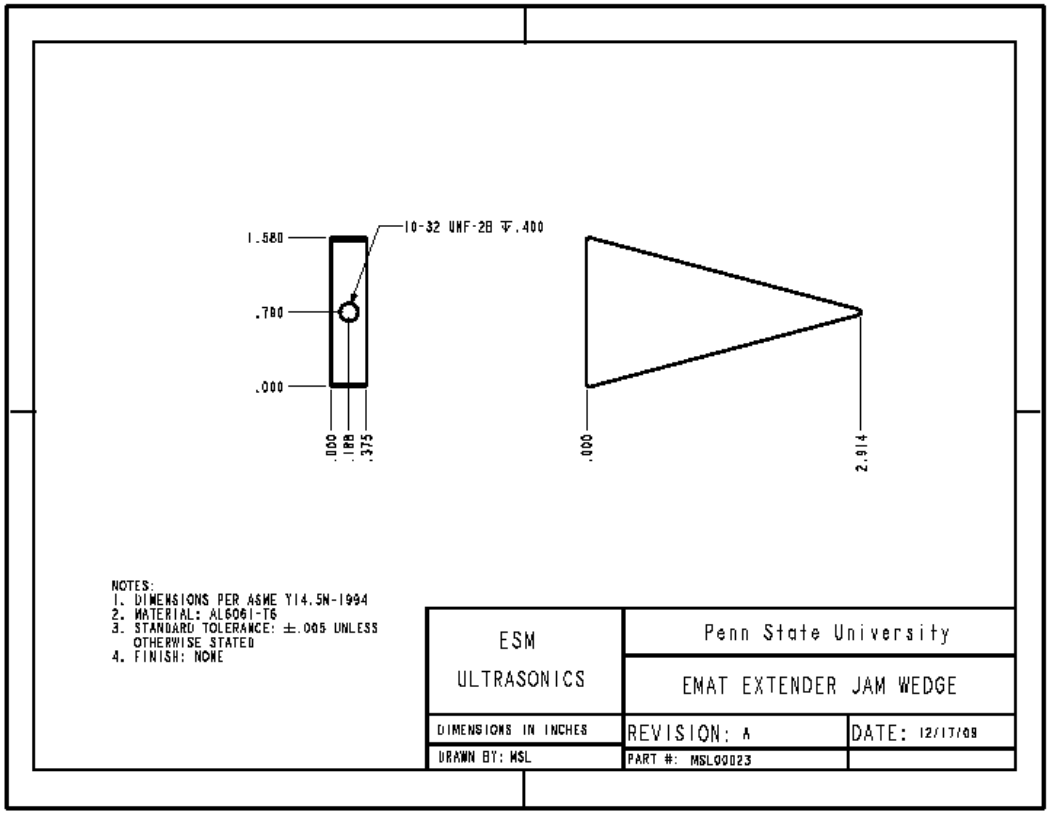
1.580
.790
.000
10-32 UNF-2B ↧.400
.000
.188
.375
.000
2.914
NOTES:
1. DIMENSIONS PER ASME Y14.5M-1994
2. MATERIAL: AL6061-T6
3. STANDARD TOLERANCE: ±.005 UNLESS OTHERWISE STATED
4. FINISH: NONE
ESM ULTRASONICS
Penn State University
EMAT EXTENDER JAM WEDGE
DIMENSIONS IN INCHES
REVISION: A
DATE: 12/17/09
DRAWN BY: MSL
PART #: MSL00023

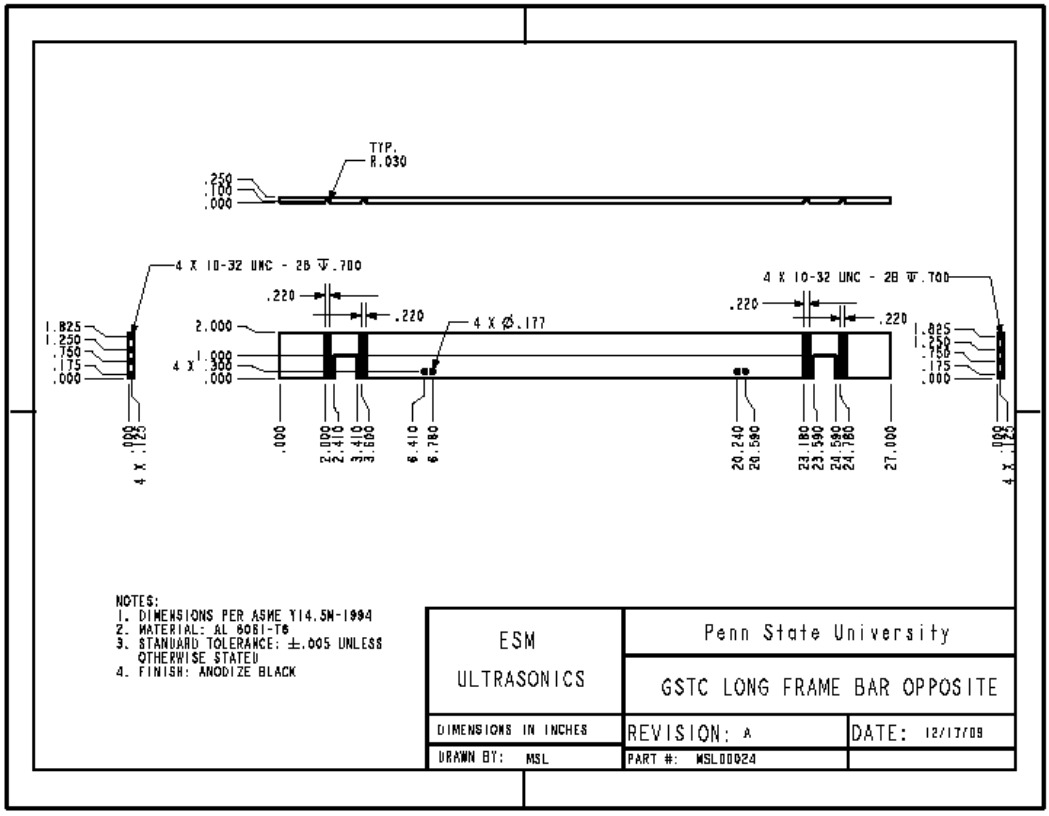
TYP.
R.030
.250
.100
.000
4 X 10-32 UNC - 2B ↧.700
.220
.220
2.000
1.000
.300
.000
4 X Ø.177
1.825
1.250
.750
.175
.000
.000
2.000
2.410
3.410
3.680
6.410
6.780
20.240
20.590
23.180
23.590
24.590
24.780
27.000
NOTES:
1. DIMENSIONS PER ASME Y14.5M-1994
2. MATERIAL: AL 6061-T6
3. STANDARD TOLERANCE: ±.005 UNLESS OTHERWISE STATED
4. FINISH: ANODIZE BLACK
ESM
ULTRASONICS
Penn State University
GSTC LONG FRAME BAR OPPOSITE
DIMENSIONS IN INCHES
REVISION: A
DATE: 12/17/09
DRAWN BY: MSL
PART #: MSL00024

Appendix B

BILLS OF MATERIALS

Bill of Materials GSTC Circumferential tool

Level	Part #	Rev	Quantity	Unit	Description	source
1	MSL00014	A	1	1	GSTC dovetail frame bar	QMAC
1	MSL00021	A	1	1	GSTC opposite dovetail frame bar	QMAC
1	MSL00016	A	2	1	GSTC end frame	Skytop Machine and Tool
1	MSL00011	A	2	1	GSTC end cap	QMAC
1	MSL00013	A	2	1	GSTC circumferential cover	QMAC
2	MSL00022	A	1	1	GSTC air cylinder mount	QMAC
2	MSL00023	A	1	1	GSTC head expander	QMAC
2	A07020SP	N/A	1	1	air cylinder	automationdirect.com
3	MSL00007	C	2	1	EMAT head housing	QMAC
3	MSL00019	A	2	1	protective urethane	Skytop Machine and Tool
3	MSL00002	B	2	1	pulser/receiver coil (must designate)	Innerspec
3	MSL00006	A	2	1	coil Lemo mount	Skytop Machine and Tool
3	280mag	A	20	1	280kHz magnet	K&J Magnetics
4	93996A721	N/A	2	1	actuation bearing shoulder bolt	McMasterCarr
4	2342K82	N/A	2	1	actuation bearing shoulder bolt	McMasterCarr
4	99154A306	N/A	8	1	wear surface bearing bolt	McMasterCarr
4	57155k364	N/A	8	1	wear surface bearing	McMasterCarr
4	92012A513	N/A	8	1	extension spring bolt	McMasterCarr
4	9654K109	N/A	4	1	1.25" lg. extension spring	McMasterCarr
4	91253A107	N/A	24	1	4-40 cover screws	McMasterCarr
4	91251A345	N/A	32	1	10-32 frame bar and cap bolts	McMasterCarr
4	91251aA194	N/A	6	1	8-32 air cylinder mount bolts	McMasterCarr
5	HM841-ND	N/A	1	1	pre-amp enclosure	Digikey
5	TR1-U2L4-0100NV1QHV-K00-S2CE	N/A	1	1	encoder	Encoder Products Company
5		N/A	1	1	PRE-AMP	FBS Inc

Level 1	**Frame components**
Level 2	**mounting/actuation parts**
Level 3	**EMAT head components**
Level 4	**Hardware**
Level 5	**Electronics**

Bill of Materials GSTC Longitudinal tool

Level	Part #	Rev	Quantity	Unit	Description	source
1	MSL00015	A	1	1	GSTC longitudinal dovetail frame bar	QMAC
1	MSL00024	A	1	1	GSTC longitudinal dovetail frame bar opposite	QMAC
1	MSL00016	A	2	1	GSTC end frame	Skytop Machine and Tool
1	MSL00011	A	2	1	GSTC end cap	QMAC
1	MSL00012	A	2	1	GSTC longitudinal cover	QMAC
2	MSL00022	A	2	1	GSTC air cylinder mount	QMAC
2	MSL00023	A	2	1	GSTC head expander	QMAC
2	A07020SP	N/A	2	1	air cylinder	automationdirect.com
3	MSL00007	C	4	1	EMAT head housing	QMAC
3	MSL00020	A	4	1	GSTC Urethane longitudinal	Skytop Machine and Tool
3	MSL00009	B	2	1	pulser/receiver coil (must designate)	Innerspec
3	MSL00006	A	4	1	coil Lemo mount	Skytop Machine and Tool
3	MSL00008	A	20	1	280kHz curved magnet	K&J Magnetics
3	MSL00010	A	20	1	280kHz curved magnet opposite pole	K&J Magnetics
4	93996A721	N/A	4	1	actuation bearing shoulder bolt	McMasterCarr
4	2342K82	N/A	4	1	actuation bearing shoulder bolt	McMasterCarr
4	99154A306	N/A	16	1	wear surface bearing bolt	McMasterCarr
4	57155k364	N/A	16	1	wear surface bearing	McMasterCarr
4	92012A513	N/A	16	1	extension spring bolt	McMasterCarr
4	9654K109	N/A	8	1	1.25" lg. extension spring	McMasterCarr
4	91253A107	N/A	24	1	4-40 cover screws	McMasterCarr
4	91251A345	N/A	32	1	10-32 frame bar and cap bolts	McMasterCarr
4	91251aA194	N/A	12	1	8-32 air cylinder mount bolts	McMasterCarr
5	HM841-ND	N/A	1	1	pre-amp enclosure	Digikey
5		N/A	1	1	PRE-AMP	FBS Inc

Level 1	**Frame components**
Level 2	**mounting/actuation parts**
Level 3	**EMAT head components**
Level 4	**Hardware**
Level 5	**Electronics**

BIBLIOGRAPHY

FBS Inc. Interview. 2007- 2011

GE Oil & Gas. Web. 15 Dec. 2010. <http://www.geoilandgas.com /businesses/ge_oilandgas/en/prod_serv/serv/pipeline/en/downloads/ geog_ultrascanduo.pdf>.

"GE Oil & Gas - Systems - Drilling & Production." GE Energy. Web. 15 Dec. 2010. <http://www.gepower.com/businesses/ge_oilandgas/en/prod_serv/systems/index.htm>.

Web. 15 Dec. 2010. <http://www.ndt-ed.org/>.

Shull, Peter J. Nondestructive Evaluation: Theory, Techniques, and Applications. New York: M. Dekker, 2002. Print.

Papavinasam, S., O. Omotoso, K. Michaelian, and R. W. Revie. "Effect of Field Operational Variables on Internal Pitting Corrosion of Oil and Gas Pipelines." *CANMET Energy Technology Centre-Devon* 65.11 (2009): 741-47. *Engineering Village*. Web. 26 Feb. 2011.

Parayitham, Sashidhar K. "Penetration Power of Ultrasonic Guided Waves for Piping and Well Casing Integrity Analysis", (Master of Science Thesis), Engineering Science and Mechanics, The Pennsylvania State University, 2008.

Program, Gas. "NETL: Oil and Natural Gas Supply." DOE - National Energy Technology Laboratory: Home Page. Web. 15 Dec. 2010. <http://www.netl.doe.gov/technologies/oil-gas/ publications/Status_Assessments/71702.pdf>.

Rose, Joseph L. Ultrasonic Waves in Solid Media. Cambridge: Cambridge UP, 1999. Print.

NaturalGas.org. Web. 03 Mar. 2011. <http://www.naturalgas.org/naturalgas/well_completion.asp>.

"EMATs." Web. 03 Mar. 2011. <http://www.ndt-ed.org/EducationResources/CommunityCollege/Ultrasonics/EquipmentTrans/emats.htm>.

Zhao, Xiaoliang, and Joseph L. Rose. "Guided Circumferential Shear Horizontal Waves in an Isotropic Hollow Cylinder." The Journal of the Acoustical Society of America 115.5 (2004): 1912. Print.